20. Flares.

Solar Flares

1. **General Observations**
2. Theoretical Models Centered on magnetic reconnection
3. Mechanisms of Particle Acceleration
4. Flare Observations in Broader Context

Why Flares?

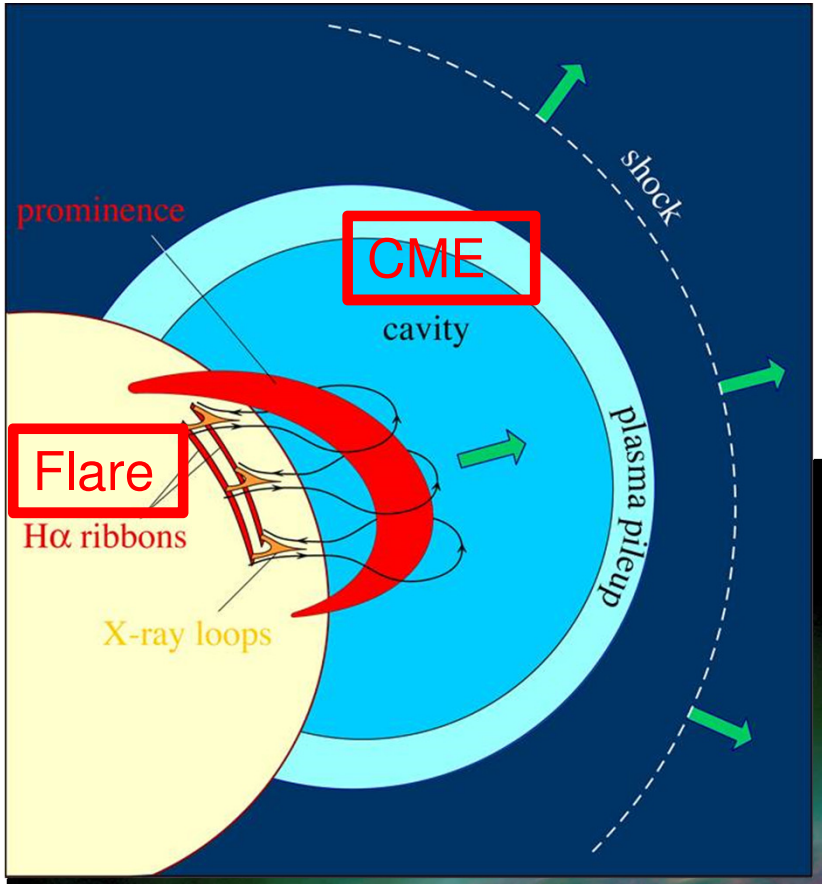
shock
prominence
CME
cavity
plasma pileup
Flare
Hα ribbons
X-ray loops

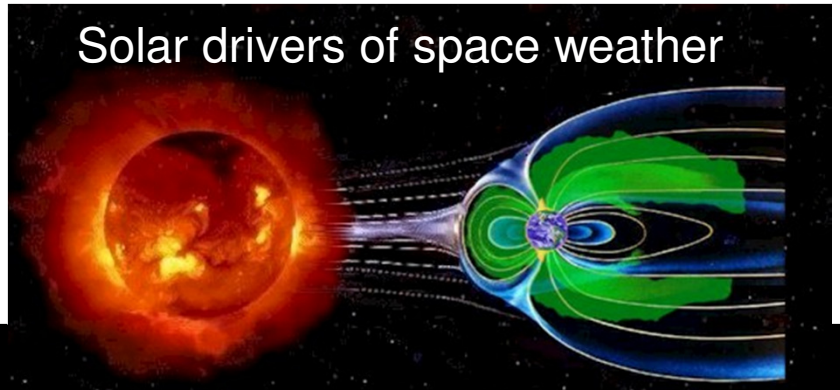
Solar drivers of space weather

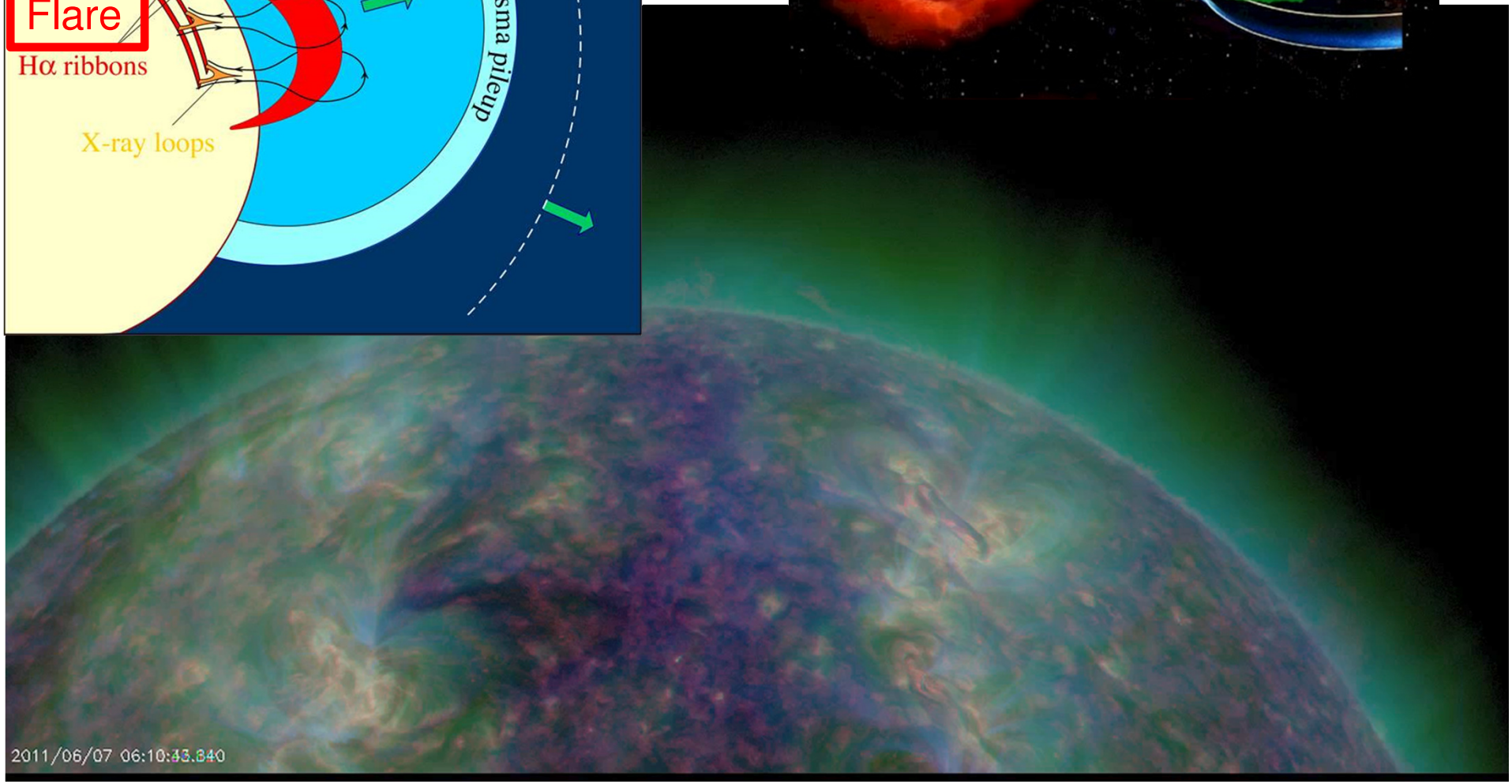
2011/06/07 06:10:43.840

AGU100 ADVANCING EARTH AND SPACE SCIENCE

Space Weather

COMMENTARY

10.1029/2018SW002024

Key Points:

- The 4 August 1972 flare, shock, and geomagnetic storm are components of a Carrington-class event
- The event was associated with a nearly instantaneous, unintended detonation of dozens of sea mines near Hai Phong, North Vietnam
- The entire series of events in August 1972 should be viewed as a grand challenge to current-day space weather models

Correspondence to:
D. J. Knipp,
delores.knipp@colorado.edu

Citation:
Knipp, D. J., Fraser, B. J., Shea, M. A., & Smart, D. F. (2018). On the little-known consequences of the 4 August 1972 ultra-fast coronal mass ejecta: Facts, commentary, and call to action. *Space Weather*, *16*. https://doi.org/10.1029/

On the Little-Known Consequences of the 4 August 1972 Ultra-Fast Coronal Mass Ejecta: Facts, Commentary, and Call to Action

Delores J. Knipp[1,2], Brian J. Fraser[3], M. A. Shea[4], and D. F. Smart[4]

[1]Smead Aerospace Engineering Sciences Department, University of Colorado Boulder, Boulder, CO, USA, [2]High Altitude Observatory, National Center for Atmospheric Research, Boulder, CO, USA, [3]Centre for Space Physics, University of Newcastle, Newcastle, NSW, Australia, [4]Retired from Air Force Research Laboratory

Abstract Today the extreme space weather events of early August 1972 are discussed as benchmarks for Sun-Earth transit times of solar ejecta (14.6 hr) and for solar energetic particle fluxes (10 MeV ion flux >70,000 $cm^{-2}{\cdot}s^{-1}{\cdot}sr^{-1}$). Although the magnetic storm index, Dst, dipped to only −125 nT, the magnetopause was observed within 5.2 R_E and the plasmapause within 2 R_E. Widespread electric- and communication-grid disturbances plagued North America late on 4 August. There was an additional effect, long buried in the Vietnam War archives that add credence to the severity of the storm impact: a nearly instantaneous, unintended detonation of dozens of sea mines south of Hai Phong, North Vietnam on 4 August 1972. The U.S. Navy attributed the dramatic event to *magnetic perturbations of solar storms*. Herein we discuss how such a finding is broadly consistent with terrestrial effects and technological impacts of the 4 August 1972 event and the propagation of major eruptive activity from the Sun to the Earth. We also provide insight into the solar, geophysical, and military circumstances of this extraordinary situation. In our view this storm deserves a scientific revisit as a grand challenge for the space weather community, as it provides space-age terrestrial observations of what was likely a Carrington-class storm.

a) Calcium Emission, 3 August 1972

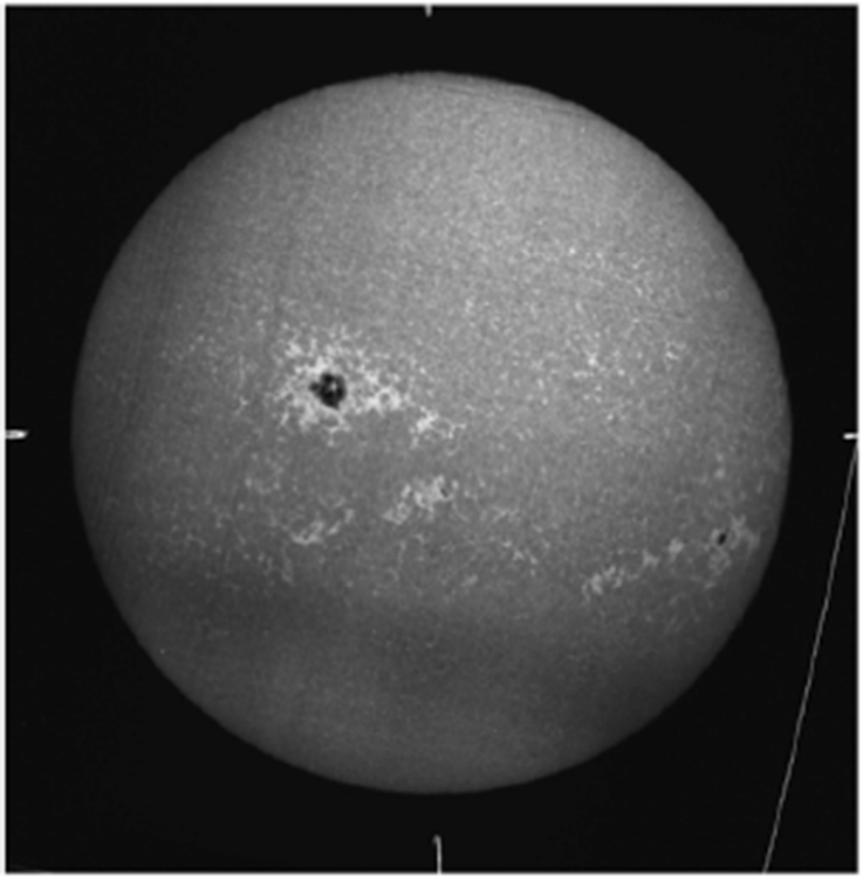

b) Hydrogen-α Emission, 4 August 1972

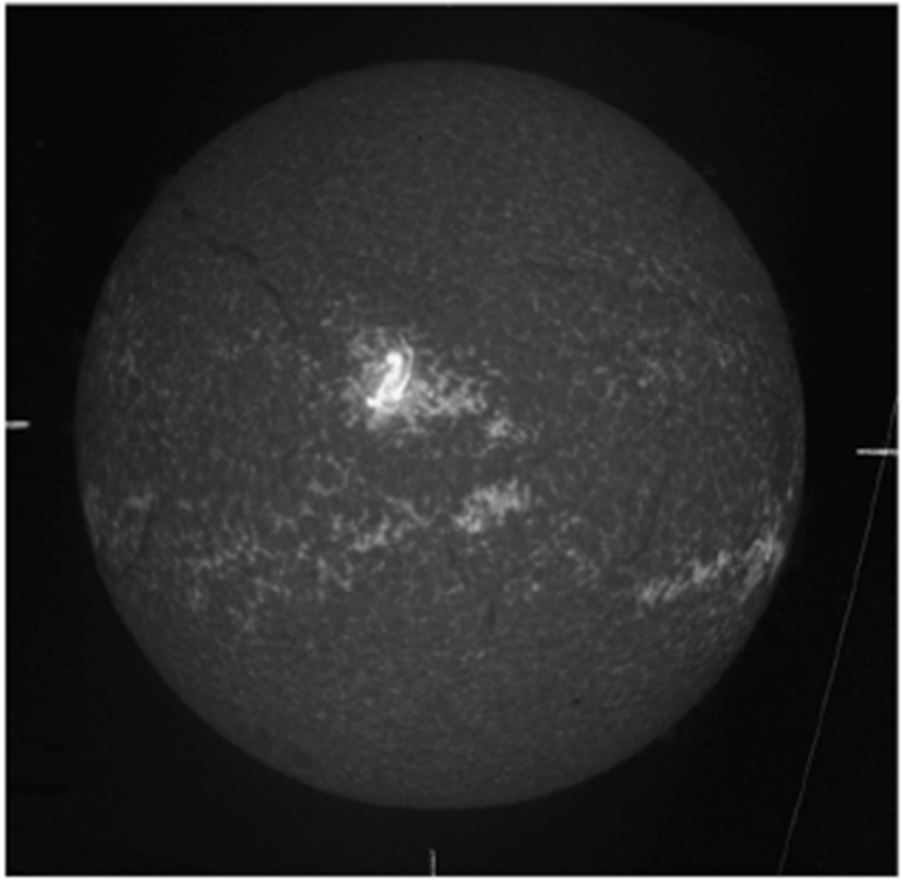

Flare - definition and classification

A solar flare is a sudden release of energy during which **via magnetic reconnection** free **magnetic energy** is converted to **kinetic energy of fast particles, mass motions, and radiation** across the entire electromagnetic spectrum.

Energy released up to **10^{25} J or 10^{32} erg in the largest solar flares**.
Many more much smaller flare-like events occur, with energies of as small as 10^{16} J – nano-flares, micro-flares etc.

GOES soft X-ray classification is most common these days.

The flux in the 1–8 Å = 0.1–0.8 nm range is recorded by this scheme:

- *B* → 10^{-7} W/m^2
- *C* → 10^{-6} W/m^2
- *M* → 10^{-5} W/m^2
- *X* → 10^{-4} W/m^2

- so an M5 flare has flux of 5×10^{-5} W/m^2.

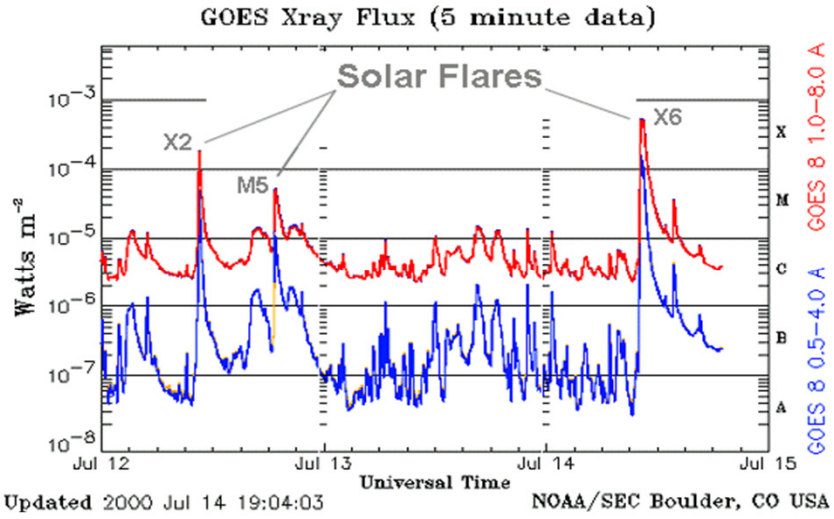

GOES = ***Geostationary Environmental Operational Satellites*** – they are continuously recording solar X-ray emission.

S. Mathews (2015)

Plasma at such high temperatures emits soft X rays through the interactions of free electrons with the nuclei (primarily protons) of the plasma. This radiation is called bremsstrahlung (from the German word meaning "braking radiation") since the radiation is produced as the electrons are deflected in the Coulomb field of the ions.

This type of emission from a plasma at a given temperature has a characteristic continuum spectrum that falls off exponentially with increasing energy, the e-folding energy being a measure of the temperature of the plasma. In an inhomogeneous plasma with a distribution of temperatures, more complicated spectral shapes are possible. Detailed spectral measurements of this emission can be used to determine the distribution of emission measure over temperature for the plasma in the emitting volume.

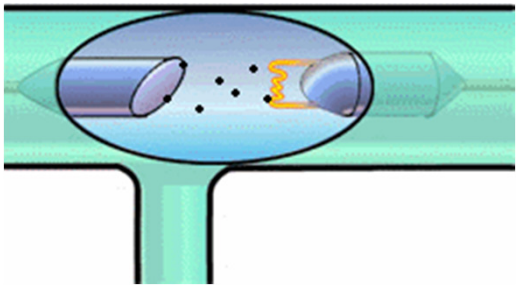

bremsstrahlung animation

The X rays and gamma rays are produced by several different processes with the result that a complex spectrum is produced involving both line and continuum emission. A composite spectrum of a large flare is shown in the figure below, where the contributions to the total emission are indicated in the different energy ranges. The longer wavelength or softer X rays from less than 1 keV to several tens of keV are produced by hot plasma with a temperature of at least 10^7 K (and possibly as high as several times 10^8 K in some cases).

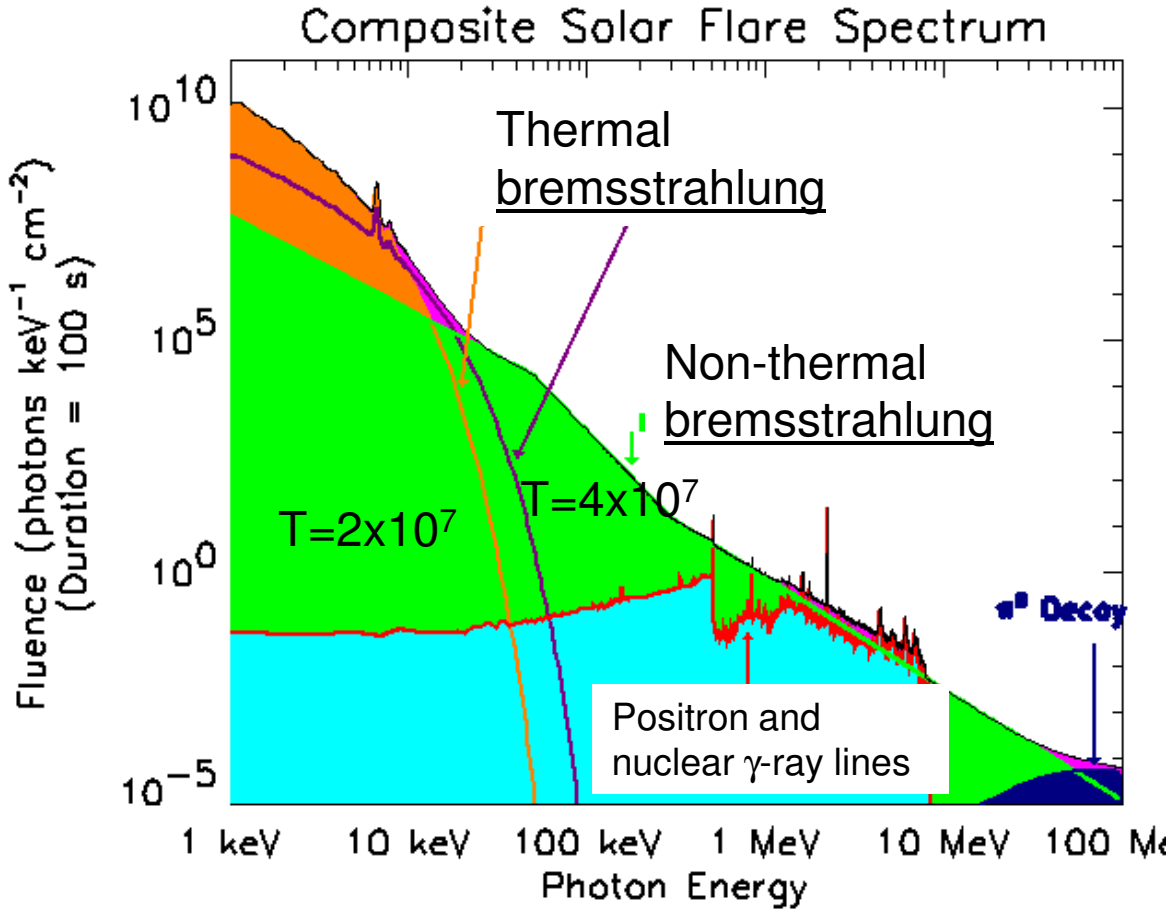

Magnetic Free Energy

The amount of magnetic energy above the potential energy that is stored and available for solar energetic events (flares, CMEs).

The total magnetic energy is calculated using full vector field measured on the surface, and assuming the force-free approximation ($\boldsymbol{j} \times \boldsymbol{B} = 0$).

Potential magnetic field is calculated using line-of-sight (vertical) magnetic field component measured on the surface, and assuming the current-free approximation ($\boldsymbol{j} = 0$).

The magnetic free energy is calculated by subtracting the potential energy from the total magnetic energy.

Flare energetics

$E_{pot} = 10^{31} - 4 \times 10^{33}$ erg

$E_{free}/E_{pot} = 0.01\text{-}0.25$

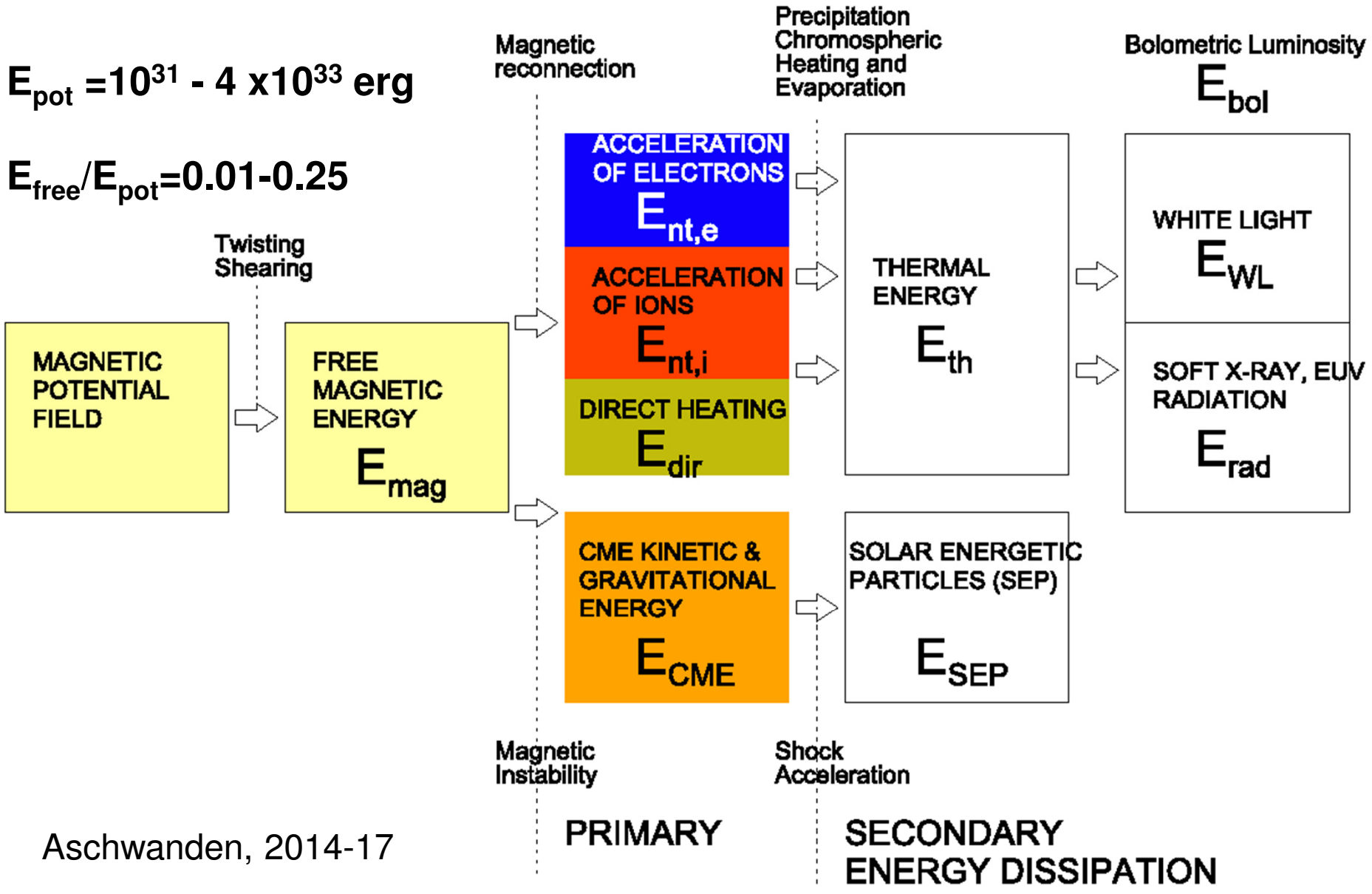

Aschwanden, 2014-17

Flare energetics

Table 13.1: Summary table of statistical energy ratios in flares. The sum of primary energies includes nonthermal electrons, ions, direct heating, and CME (kinetic and potential) energies (Aschwanden et al. 2017).

Energy type type	Number of flares	Fraction of energies
Free magnetic energy	172	$E_{\rm mag}/E_{\rm mag} = 1.00 \pm 0.00$
Nonthermal electrons	55	$E_{\rm nt,e}/E_{\rm mag} = 0.51 \pm 0.17$
Nonthermal ions	55	$E_{\rm nt,i}/E_{\rm mag} = 0.17 \pm 0.17$
CME energy	157	$E_{\rm CME}/E_{\rm mag} = 0.07 \pm 0.14$
SEP energy	4	$E_{\rm SEP}/E_{\rm mag} = 0.10 \pm 1.64$
Direct heating	106	$E_{\rm dir}/E_{\rm mag} = 0.07 \pm 0.17$
Thermal energy	170	$E_{\rm th}/E_{\rm mag} = 0.08 \pm 0.13$
Radiated energy in SXR	171	$E_{\rm rad}/E_{\rm mag} = 0.004 \pm 0.130$
Bolometric energy	172	$E_{\rm bol}/E_{\rm mag} = 0.07 \pm 0.10$
Sum of primary energies	52	$E_{\rm sum}/E_{\rm mag} = 0.87 \pm 0.18$
Thermal energy	391	$E_{\rm th}/E_{\rm th} = 1.00 \pm 0.00$
Radiated energy in SXR	389	$E_{\rm rad}/E_{\rm th} = 0.07 \pm 0.06$
Bolometric energy	391	$E_{\rm bol}/E_{\rm th} = 1.14 \pm 0.05$


Apr 17 2002 23:59:32

Global Coronal Response to Flare+CME eruption

Utilize multiple EUV channels' sensitive thermal response

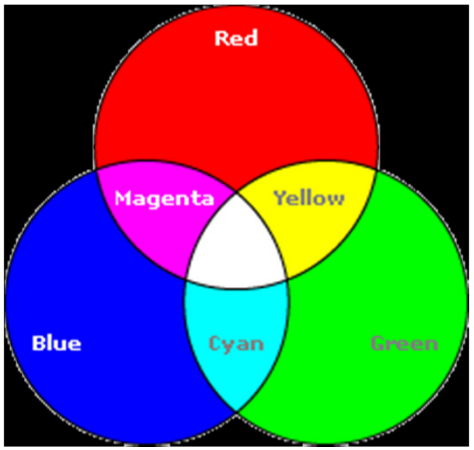

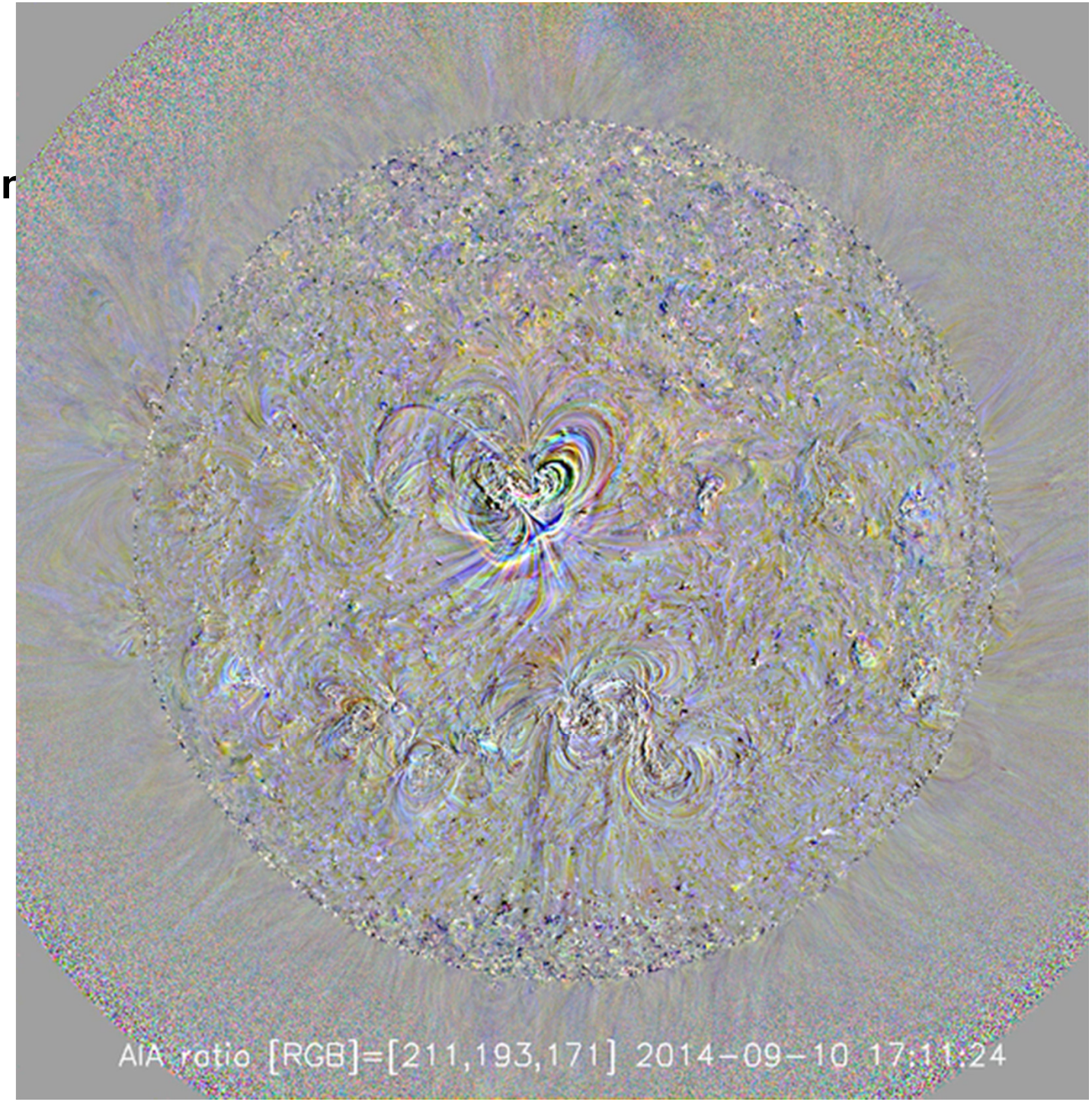

Observations – two-ribbon flare picture

Flares release energy in many forms - electro-magnetic (Gamma rays and X-rays), energetic particles (protons and electrons), and mass flows. Solar flares are often observed using H-alpha 6563 Angstrom filters. Most solar observatories have H-alpha telescopes and some observatories monitor the Sun for solar flares by capturing images of the Sun every few seconds.

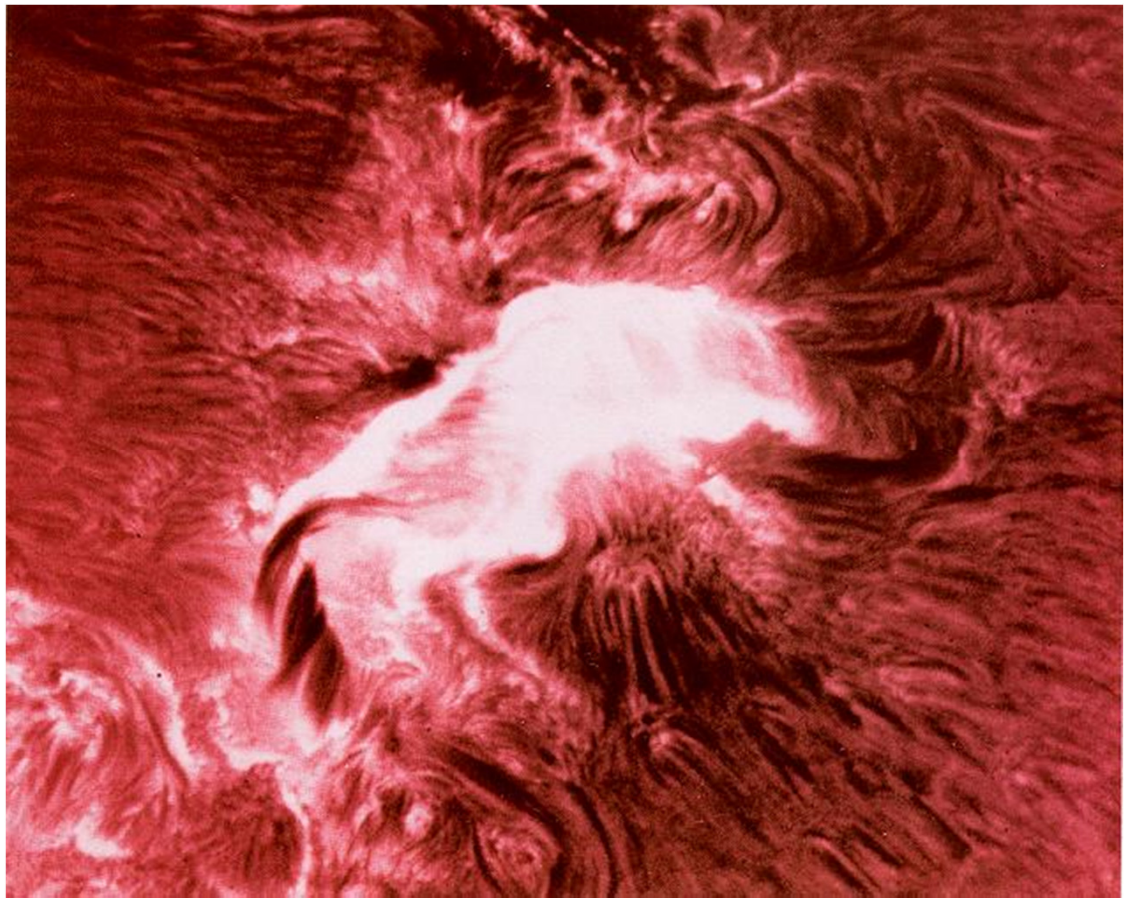

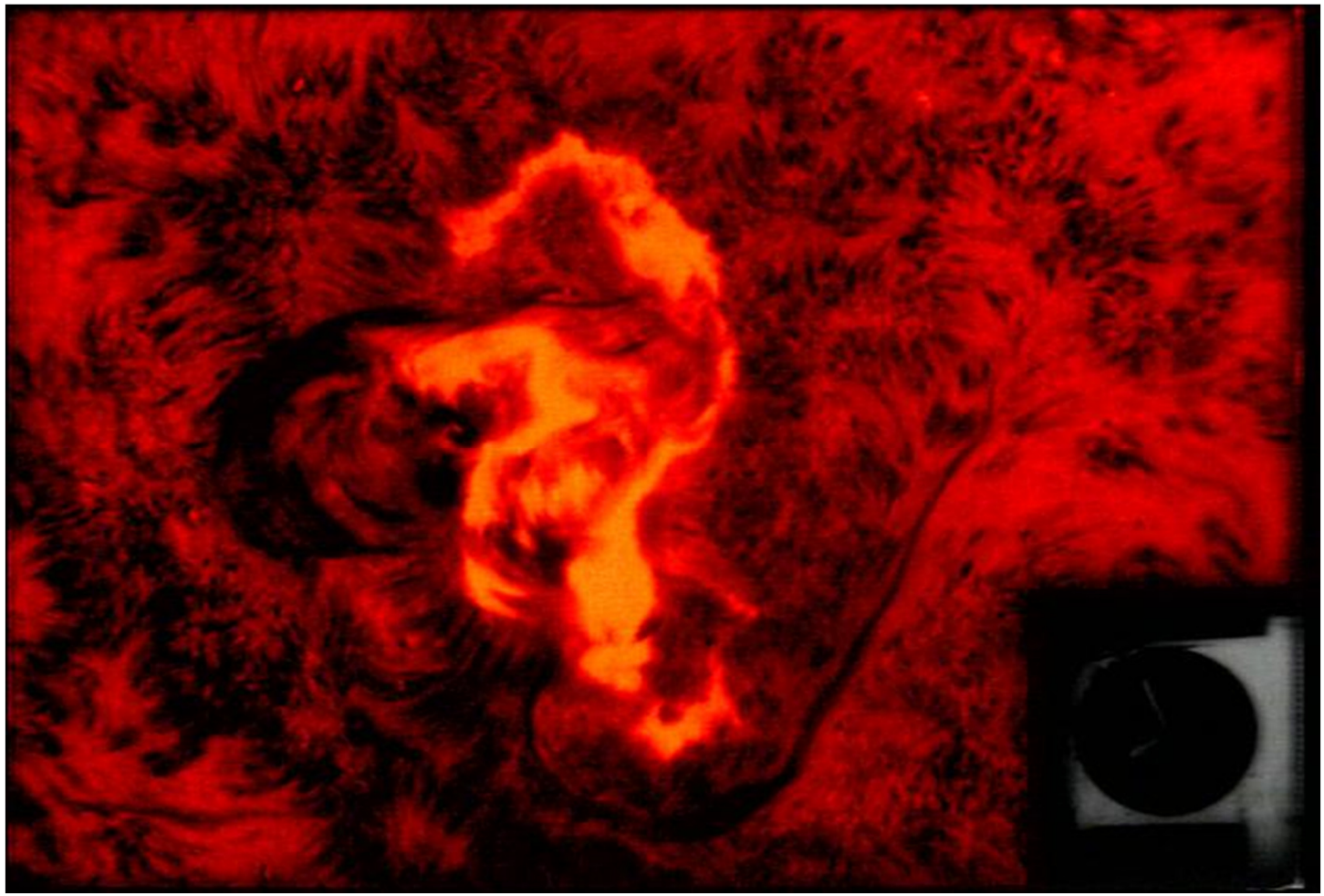

The image at the lower left shows a powerful flare observed on the disk of the Sun on August 7th, 1972. This is an example of a "two-ribbon" flare in which the flaring region appear as two bright lines threading through the area between sunspots within a sunspot group


Solar Flare
1972 August 07
Big Bear Solar Observatory

Solar flares occur near sunspots, usually along the dividing line (neutral line) between areas of oppositely directed magnetic fields. The two-ribbon structure is associated with footpoints of a magnetic arcade.

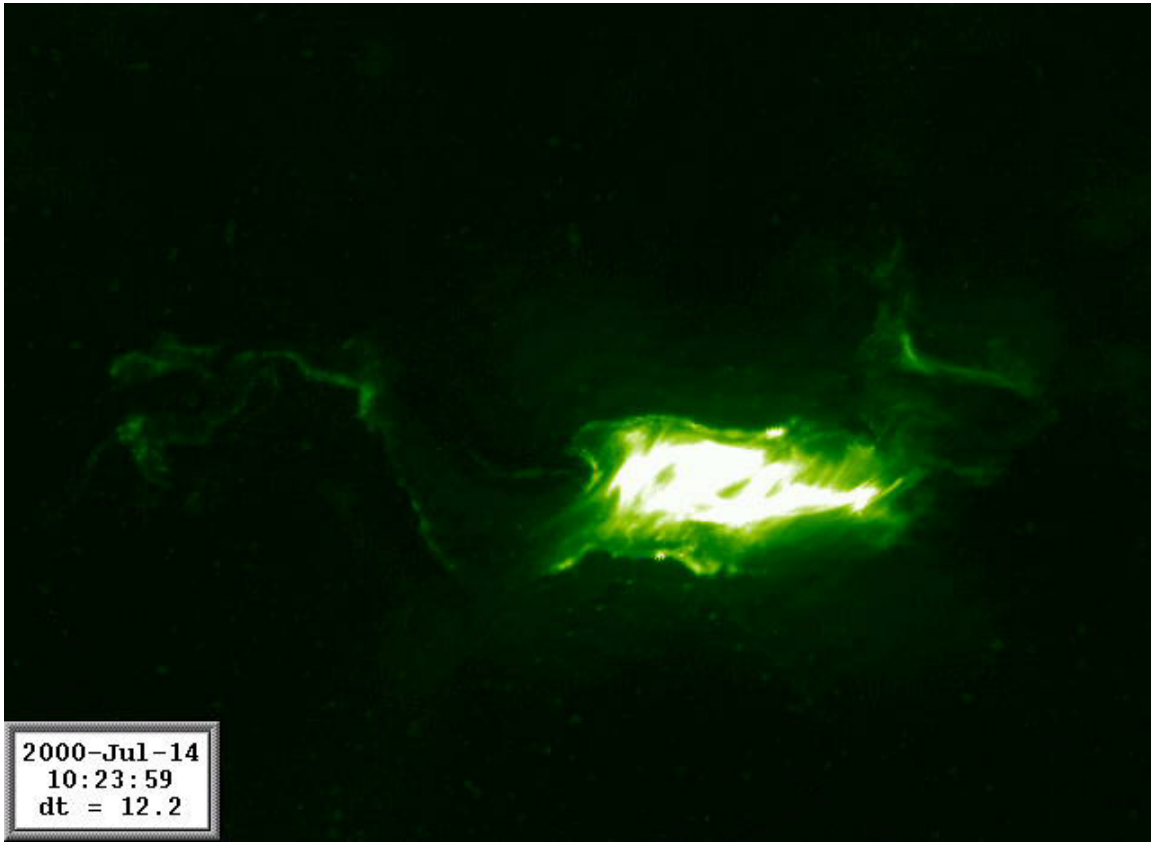

An EUV image of a solar flare of July 14, 2000, obtained by TRACE in 171Å line. The flare started at 10:10 UT.

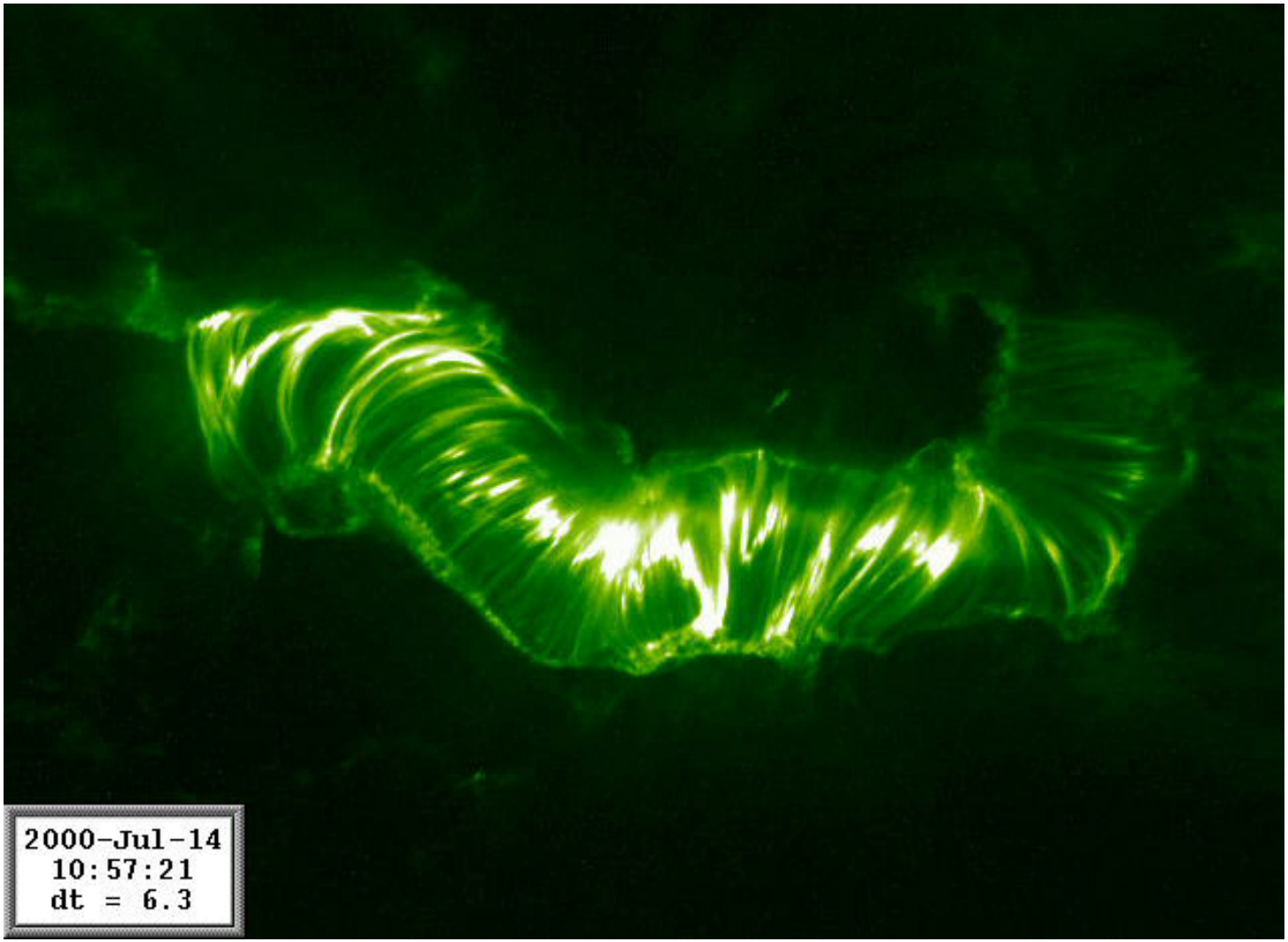

An EUV image of postflare loops in 171Å line.

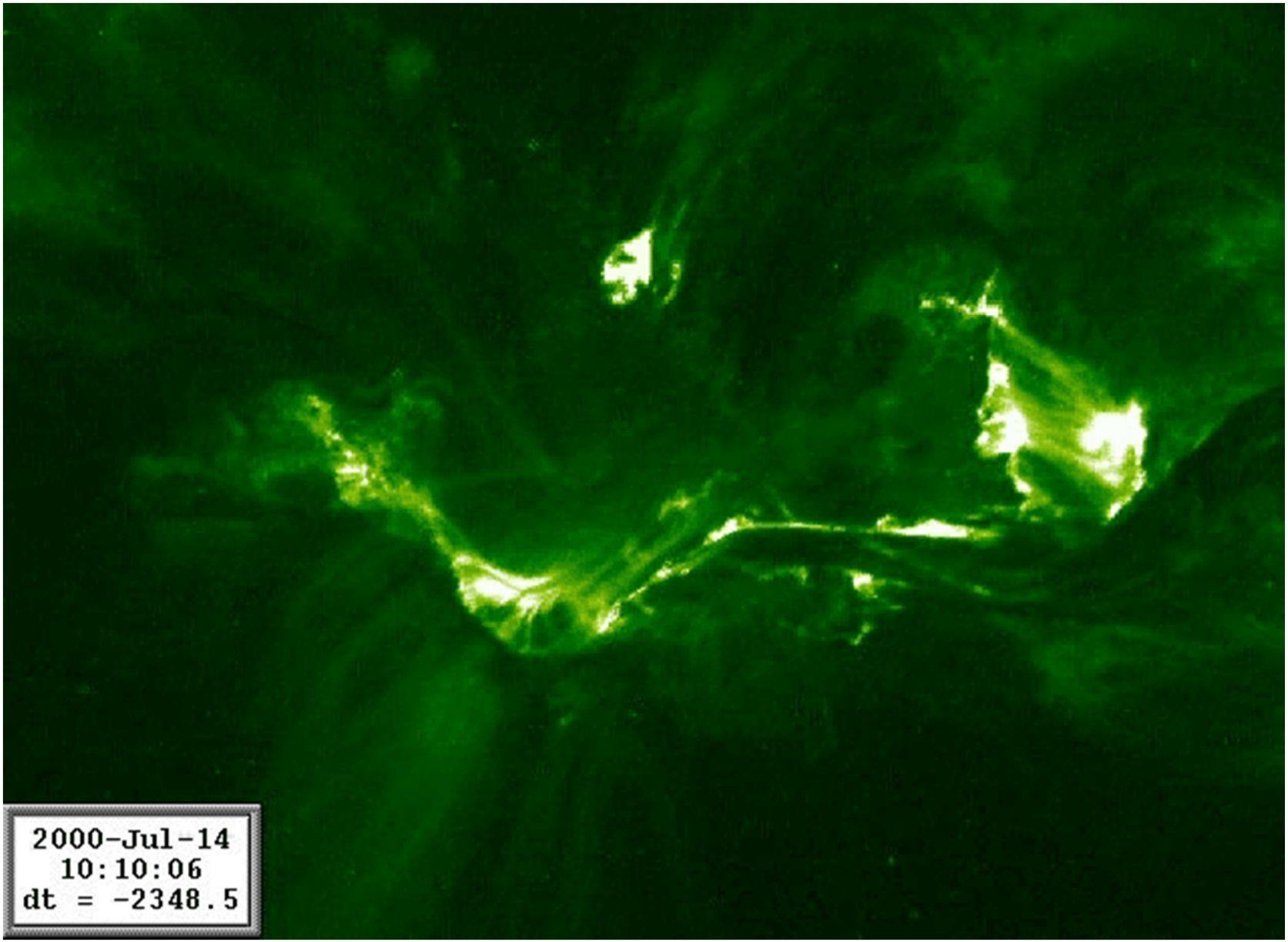
2000-Jul-14
10:10:06
dt = -2348.5

Flares and magnetic fields

The key to understanding and predicting solar flares is the structure of the magnetic field around sunspots. If this structure becomes twisted and sheared then magnetic field lines can cross and reconnect with the explosive release of energy. In the image to the left the blue lines represent the neutral lines between areas of oppositely directed magnetic fields. Normally the magnetic field would loop directly across these lines from positive (outward pointing magnetic field) to negative (inward pointing magnetic field) regions.

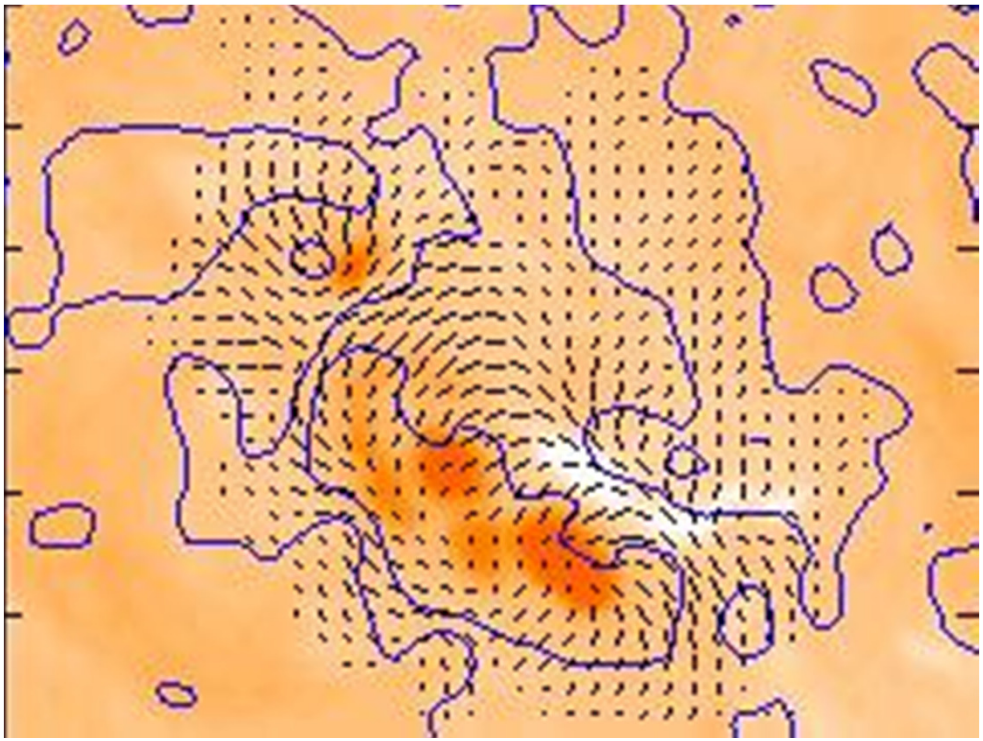

Magnetic field structure in a solar flare of June 10, 1991. The solid lines are "neutral lines" that separate areas with opposite magnetic polarity (positive from negative or north from south). The tickmarks point in the direction of the horizontal, or transverse, component of the magnetic field. Normally the transverse field is directed across (or perpendicular to) the neutral lines so that the magnetic field lines travel from the positive polarity regions directly to the negative polarity regions. In this example we see several areas where the tickmarks are directed almost parallel to the neutral lines. The magnetic field is said to be sheared in these regions. The corresponding H-alpha image is in the background.

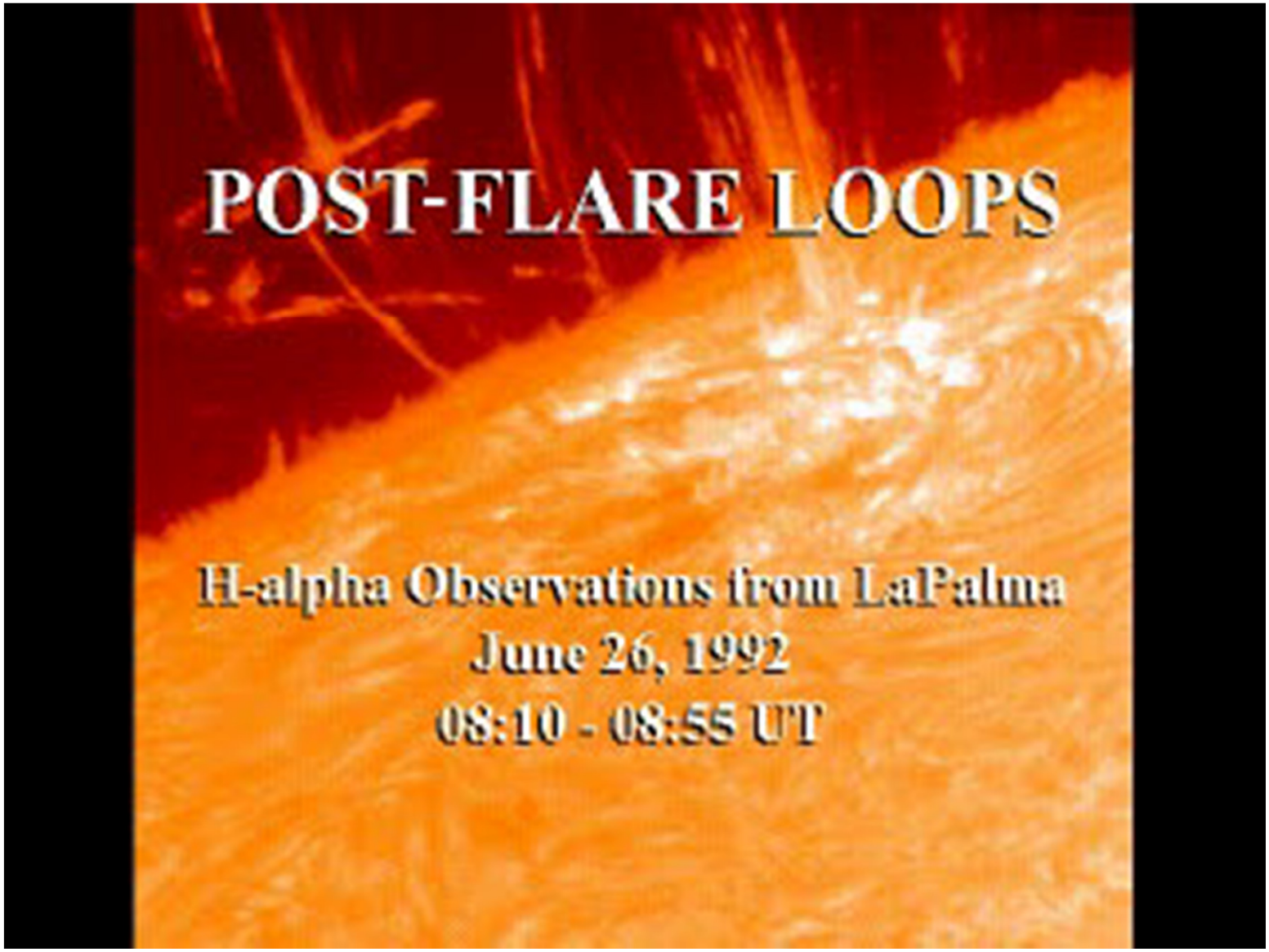
POST-FLARE LOOPS
H-alpha Observations from LaPalma
June 26, 1992
08:10 - 08:55 UT

A soft X-ray image of a solar flare from YOHKOH

Flare Phases

During a large solar flare, the X-ray and gamma-ray flux is observed to increase by many orders of magnitude over preflare levels. Indeed, preflare fluxes are not detectable at energies above 10 - 20 keV. The time profile at several different energies for a large flare on 6 March, 1989, is shown below.

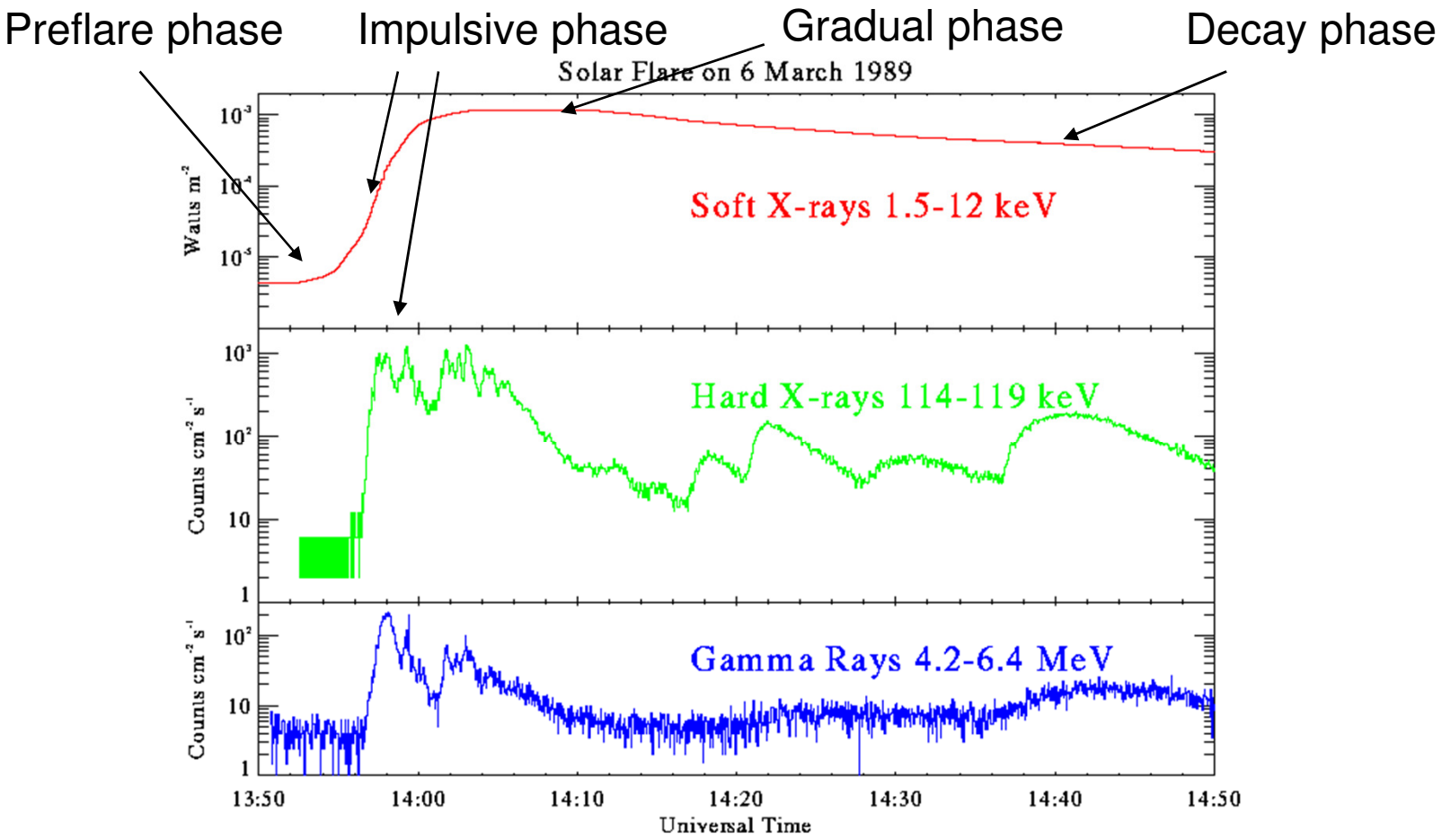

The following different stages can be recognized from this plot:

1. The **preflare stage** from about 13:50 to 13:56 UT in which the soft X-ray emission gradually increases but little if any hard X rays or gamma rays are detected above the instrumental background level.

Preflare phase

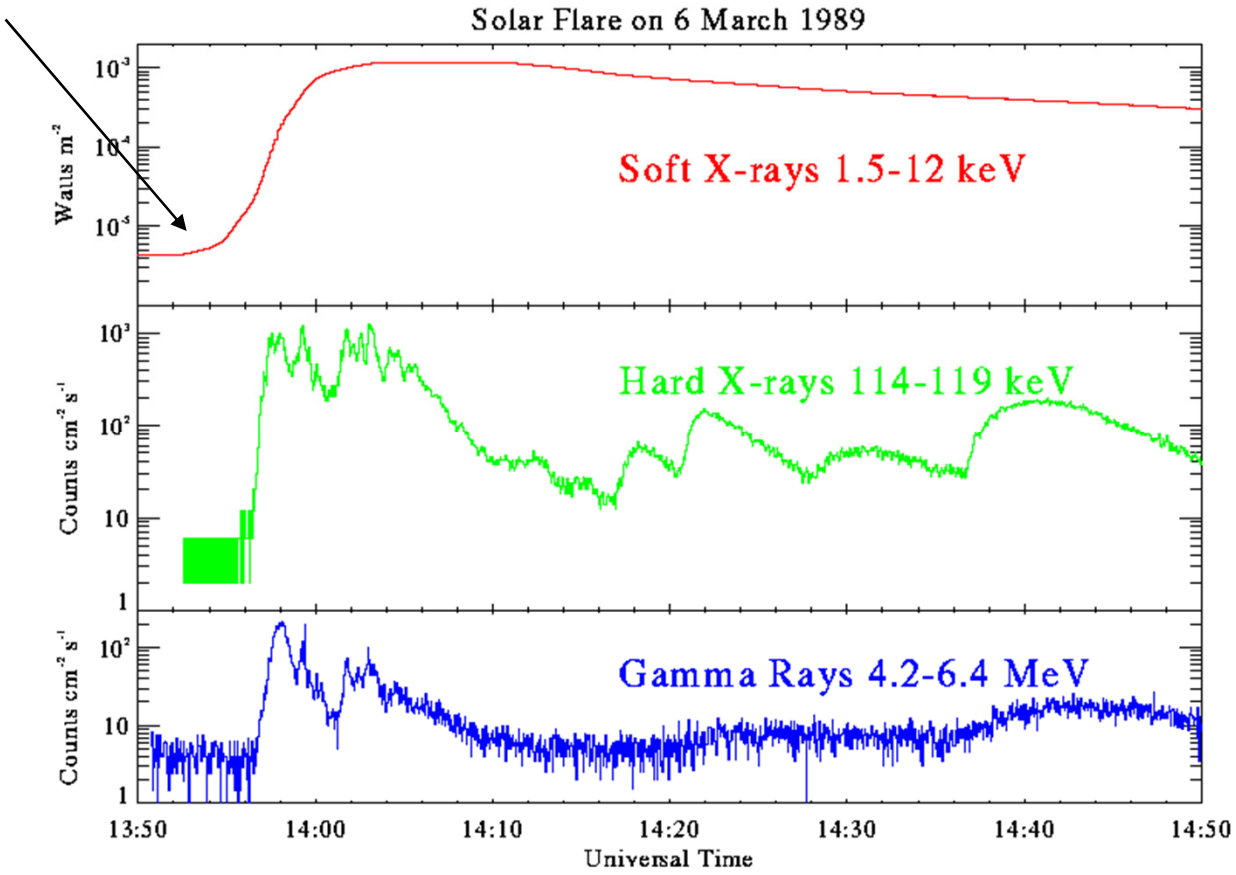

2. This is followed by the so-called **impulsive phase** in which the hard X-ray and gamma-ray emission rises impulsively, often with many short but intense spikes of emission, each lasting a few seconds to tens of seconds. The soft X-ray flux rises more rapidly during this phase with its time profile roughly matching the time integral of the hard X-ray profile in many cases.

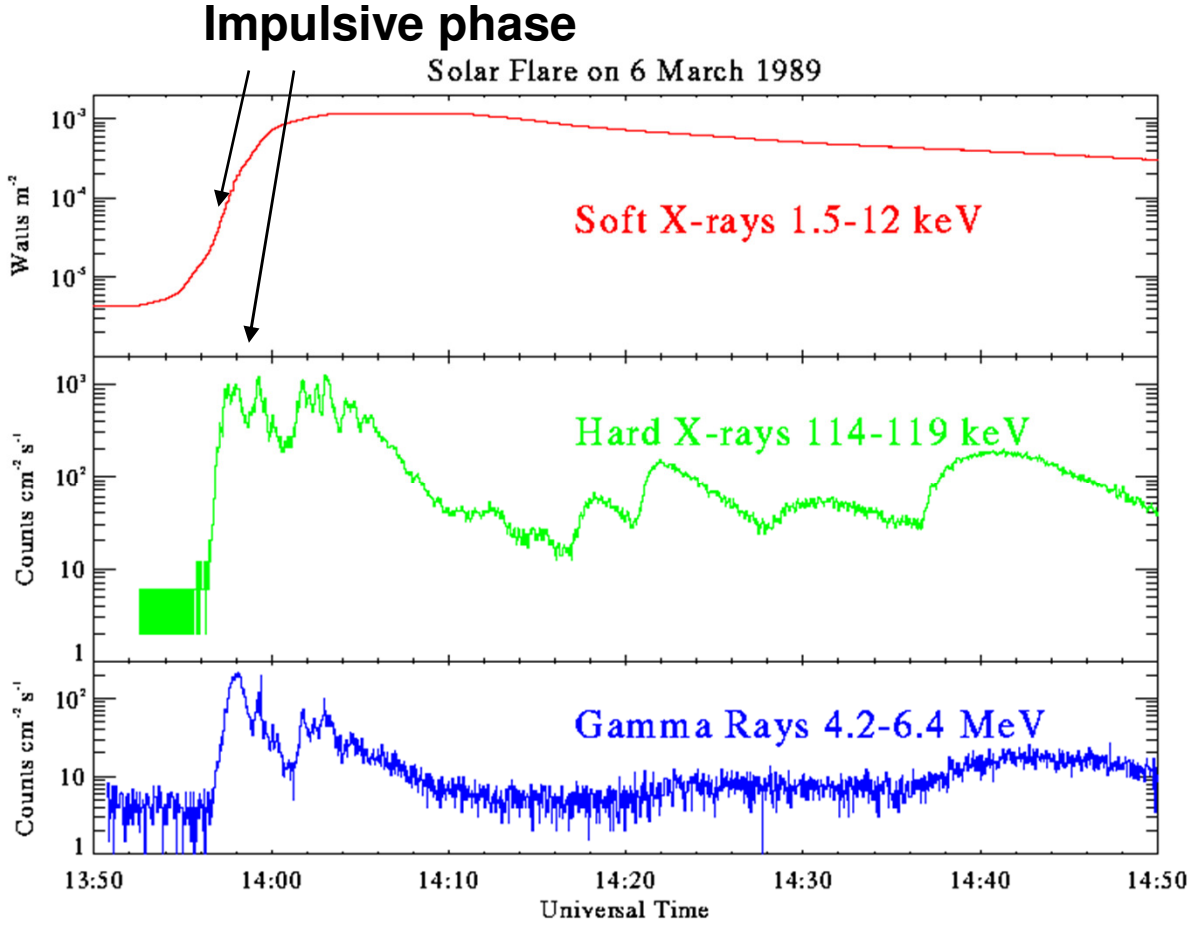

3. After about 14:06 UT the **gradual phase** begins, and the hard X-ray and gamma-ray fluxes start to decay away more or less exponentially with a time constant of minutes. The soft X-ray flux continues to rise to a later peak and then it too falls exponentially but with a significantly longer time constant, sometimes as long as several hours.

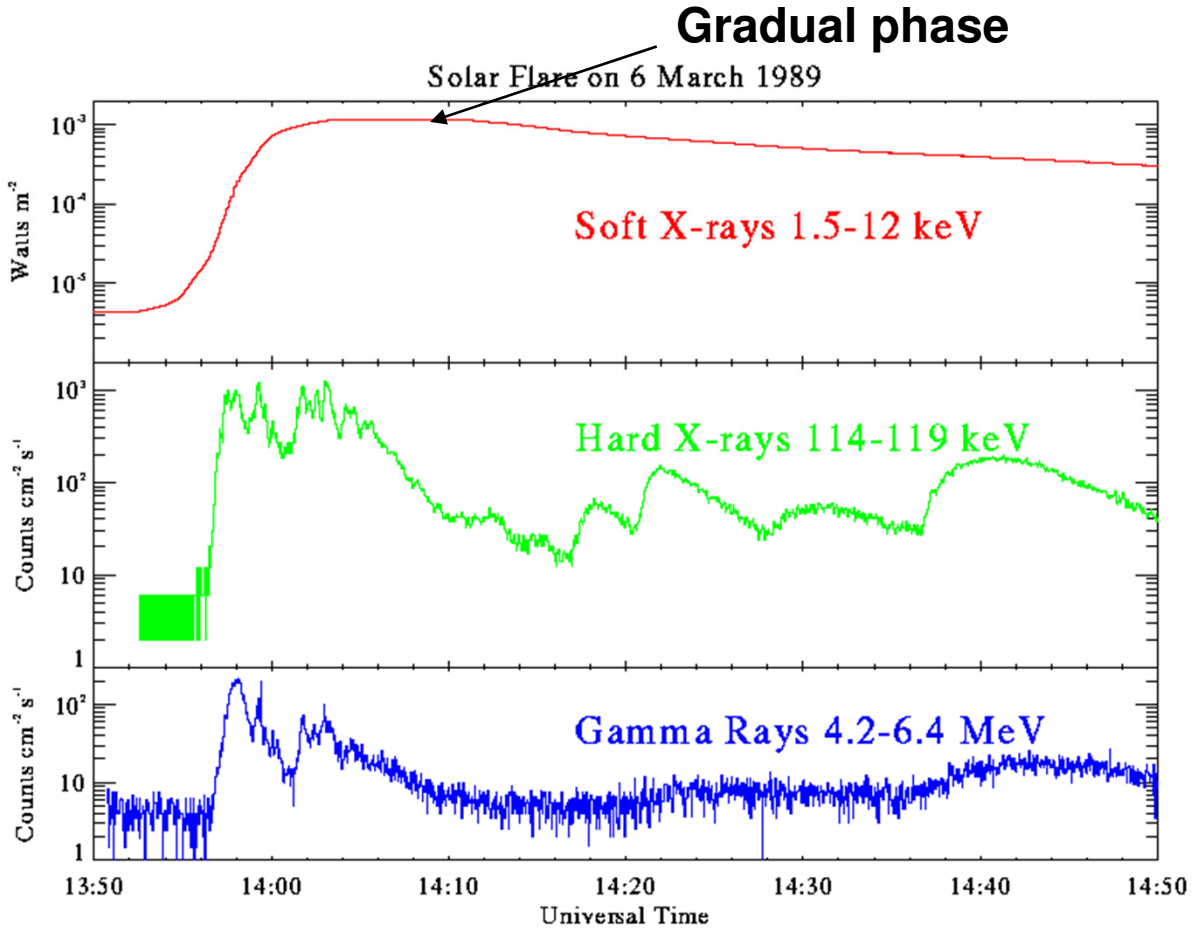

4. In this particular flare, a second phase of hard X-ray and gamma-ray emission occurs after about 14:10 UT in which the fluxes vary more gradually than during the impulsive phase. This later, more gradual phase of high energy emissions is not detected in most flares. Note that the soft X-ray flux continues to fall smoothly during this **decay phase**.

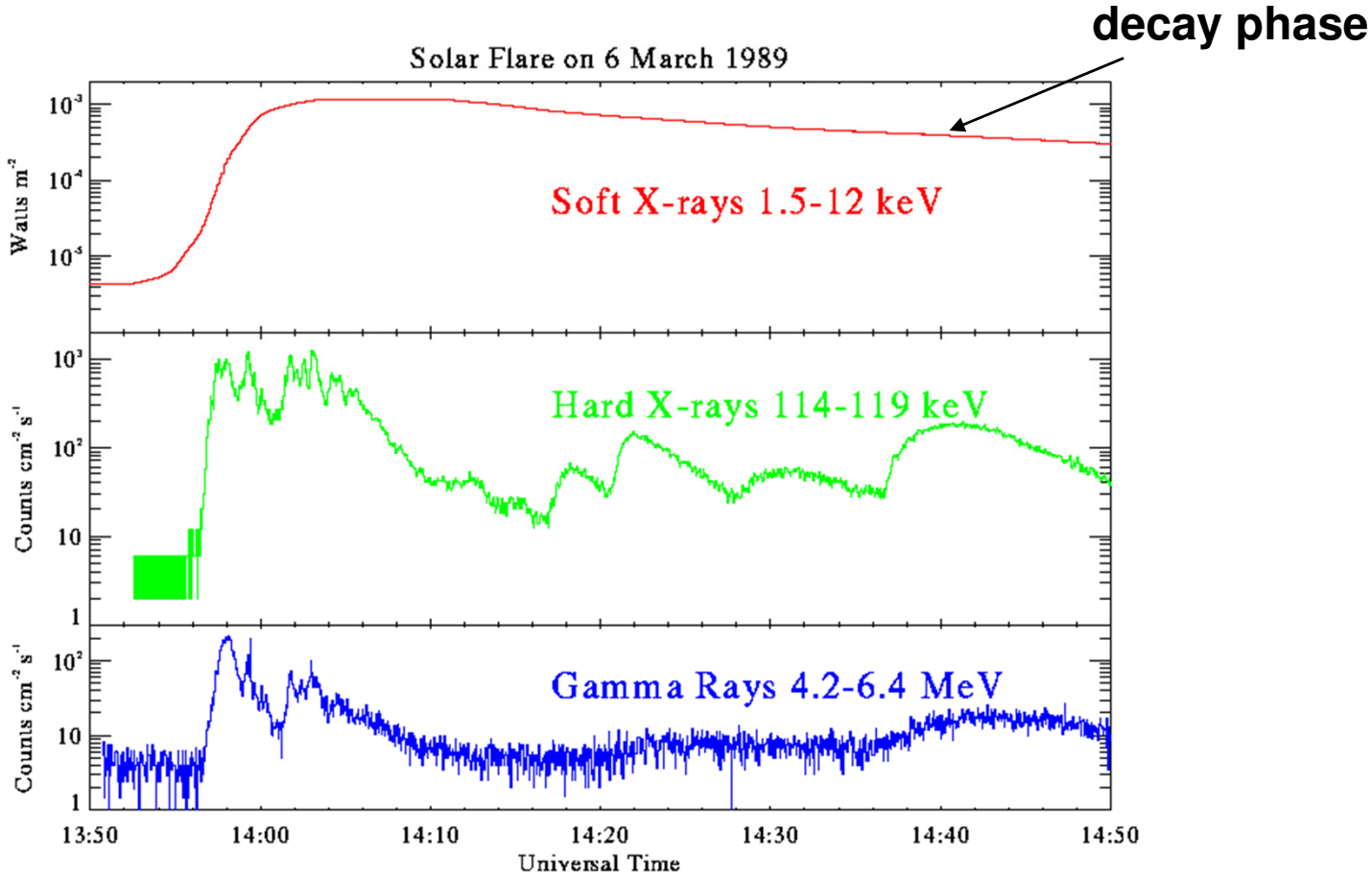

The Neupert Effect: The soft X-ray curve corresponds to the integral of the hard X-ray curve.

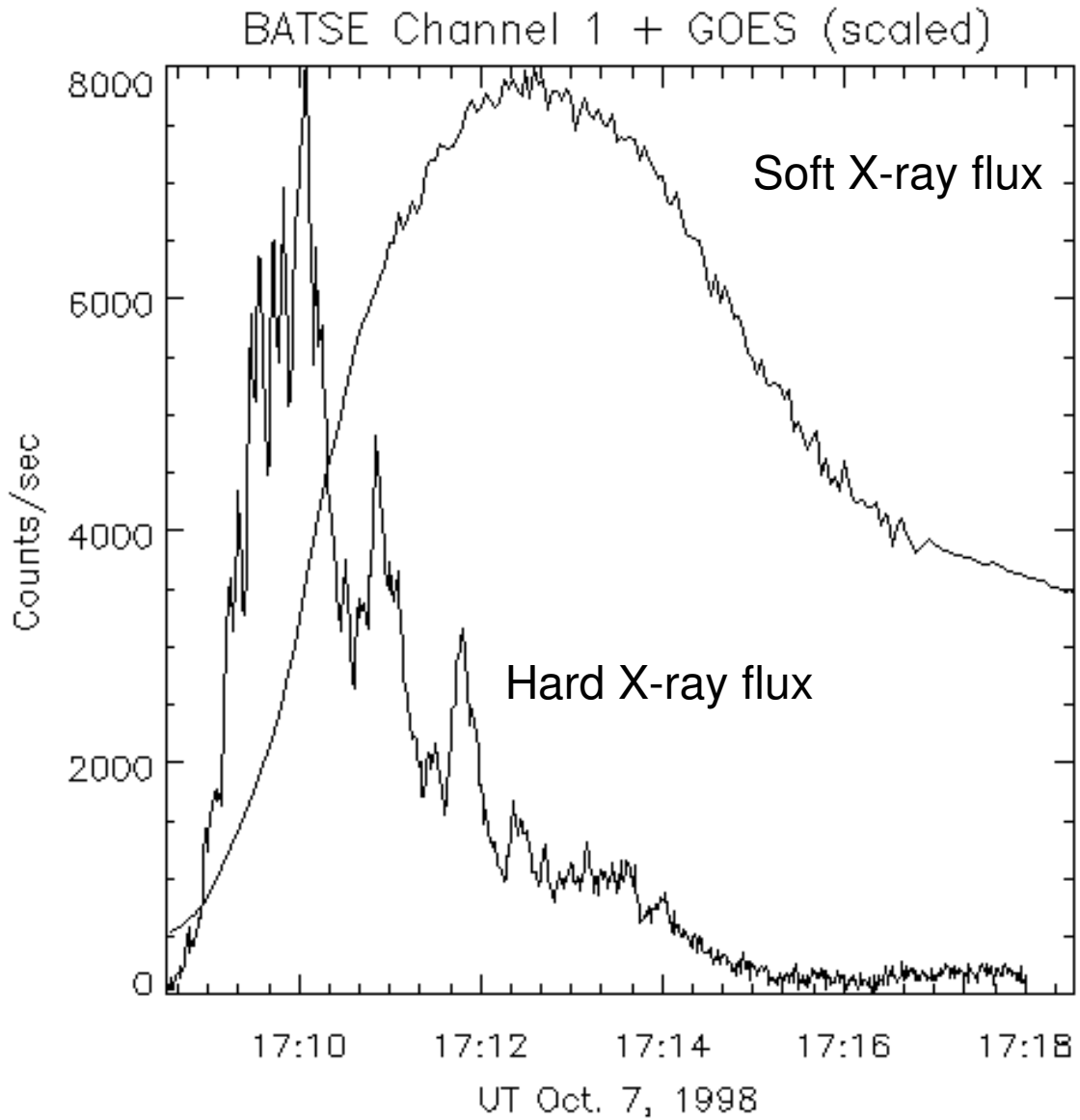

The Neupert Effect. This shows the soft X-ray light curve of the flare (from the GOES soft channel), together with the hard X-ray light curve from CGRO/BATSE. The BATSE "channel 1" counts (nominally 25-50 keV) are roughly equivalent to the Yohkoh HXT M2 channel (nominally 33-53 keV). The GOES light curve is normalized arbitrarily to BATSE. The Neupert effect simply notes that the hard X-rays occur during the rise phase of the soft X-rays. This general pattern is what one would expect if the hard X-ray flux somehow accompanied the energy release phase in the flare, when the hot plasma is building up in the coronal loops.

Sympathetic Solar Flares

Trigger sympathetic eruptions

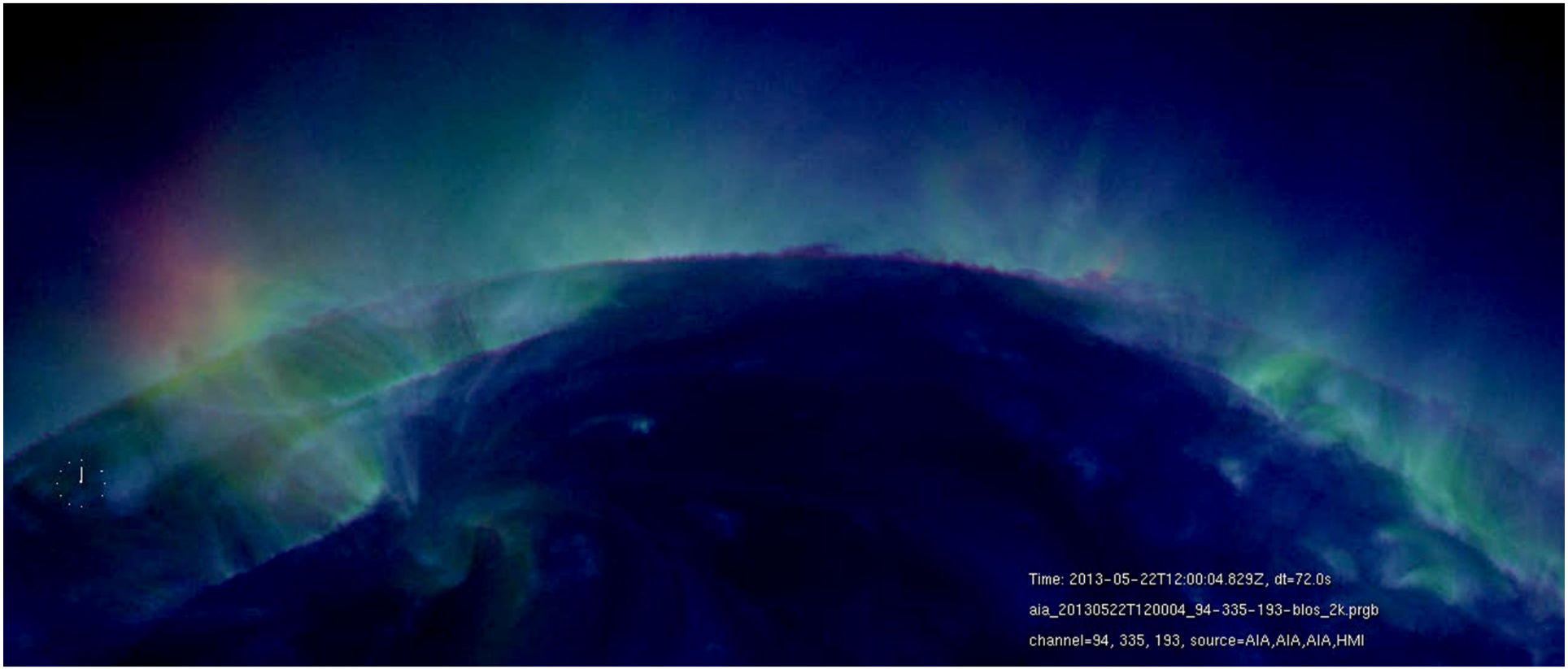

A variety of evidence suggests that the energy release mechanism in flares is fragmentary, involve multiple small-scale energy release events that trigger one another. Large numbers ($\sim 10^4$) of microwave spike bursts are observed in some flares, which may correspond to individual energy release events.

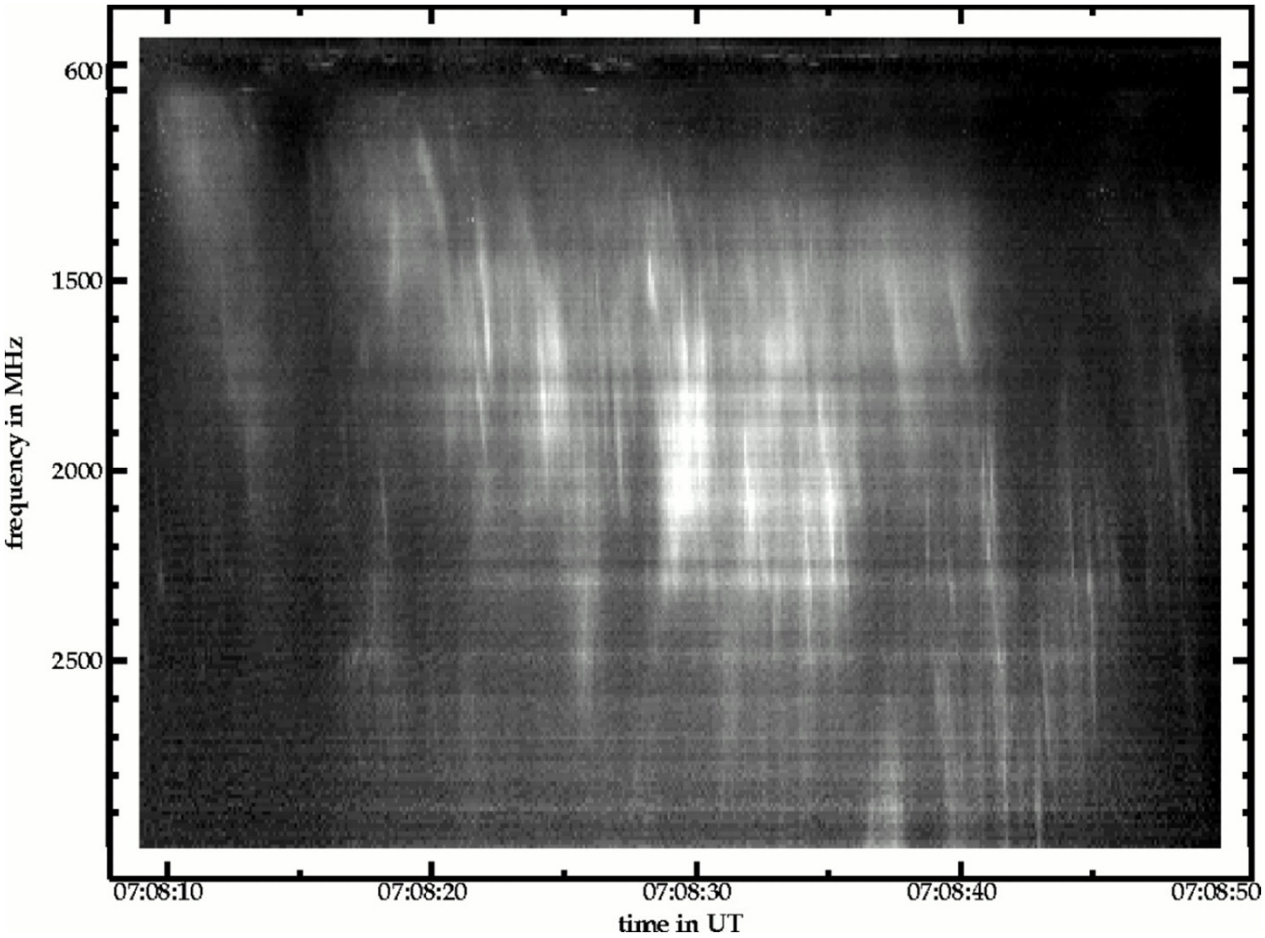

Hundreds of decimetric (type III) radio bursts produced during a flare by electrons moving down in the corona.

Solar Flares

1. General Observations
2. **Theoretical Models Centered on magnetic reconnection**
3. Mechanisms of Particle Acceleration
4. Flare Observations in Broader Context

Solar flares – standard model

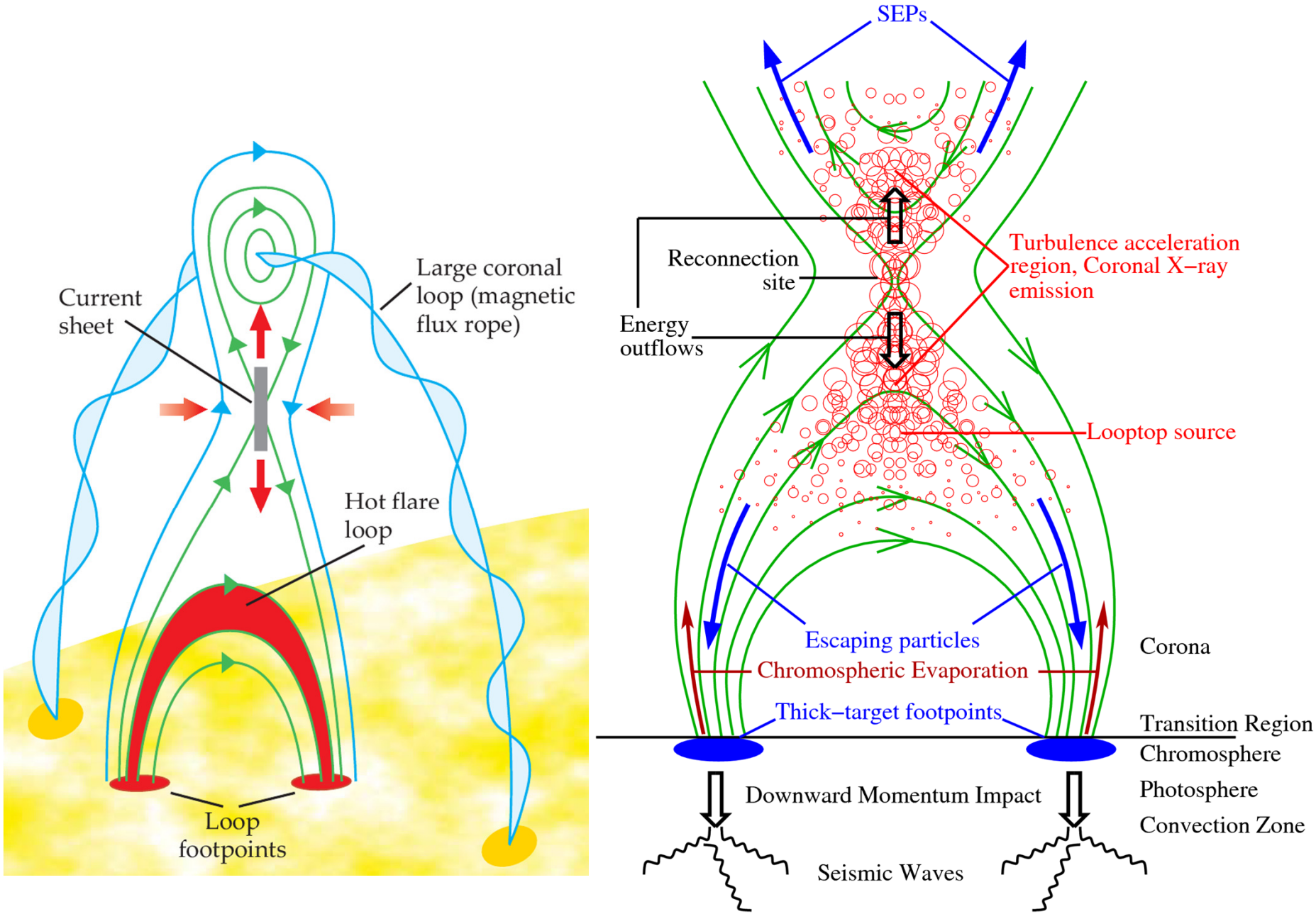

Theoretical Models

It is difficult to explain the rapid release of magnetic energy in flares because the diffusion timescale is enormously long for values of the coronal conductivity and length scales typical of active regions. Two possible solutions to this problem are first that energy release occurs where the spatial scale for variation of the magnetic field is small, and second that the resistivity of coronal plasma may be enhanced by plasma instabilities.

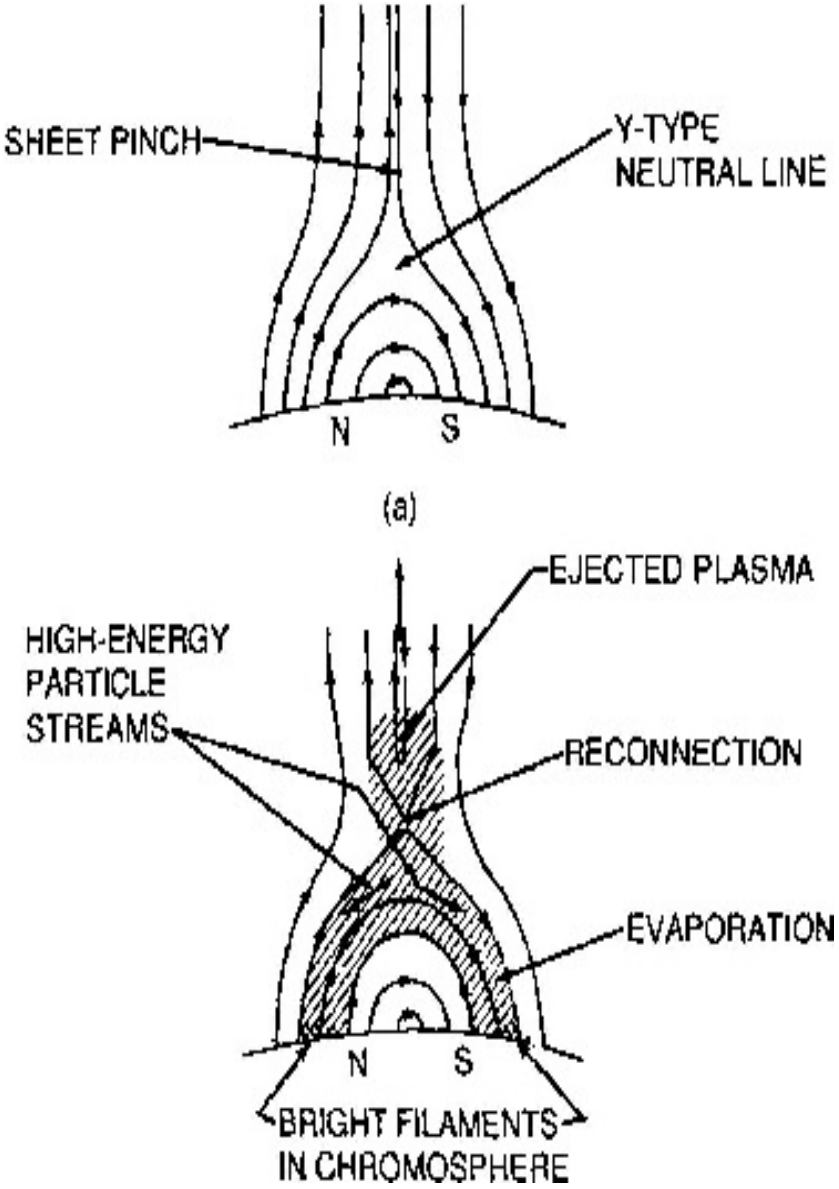

Arcade-type flares are often explained in terms of a "standard model" involving reconnection occurring high in the corona. The figure below shows a variant of the standard model, due to Sturrock. The evidence for reconnection high in the corona is that gradual flares often involve cusped soft X-ray loops, suggestive of a 2-D current sheet configuration above the loops. The spreading of H-alpha ribbons is also naturally explained in terms of reconnection at a rising location in the overlying corona.

Small flares are thought to be caused by reconnection with new emerging flux.

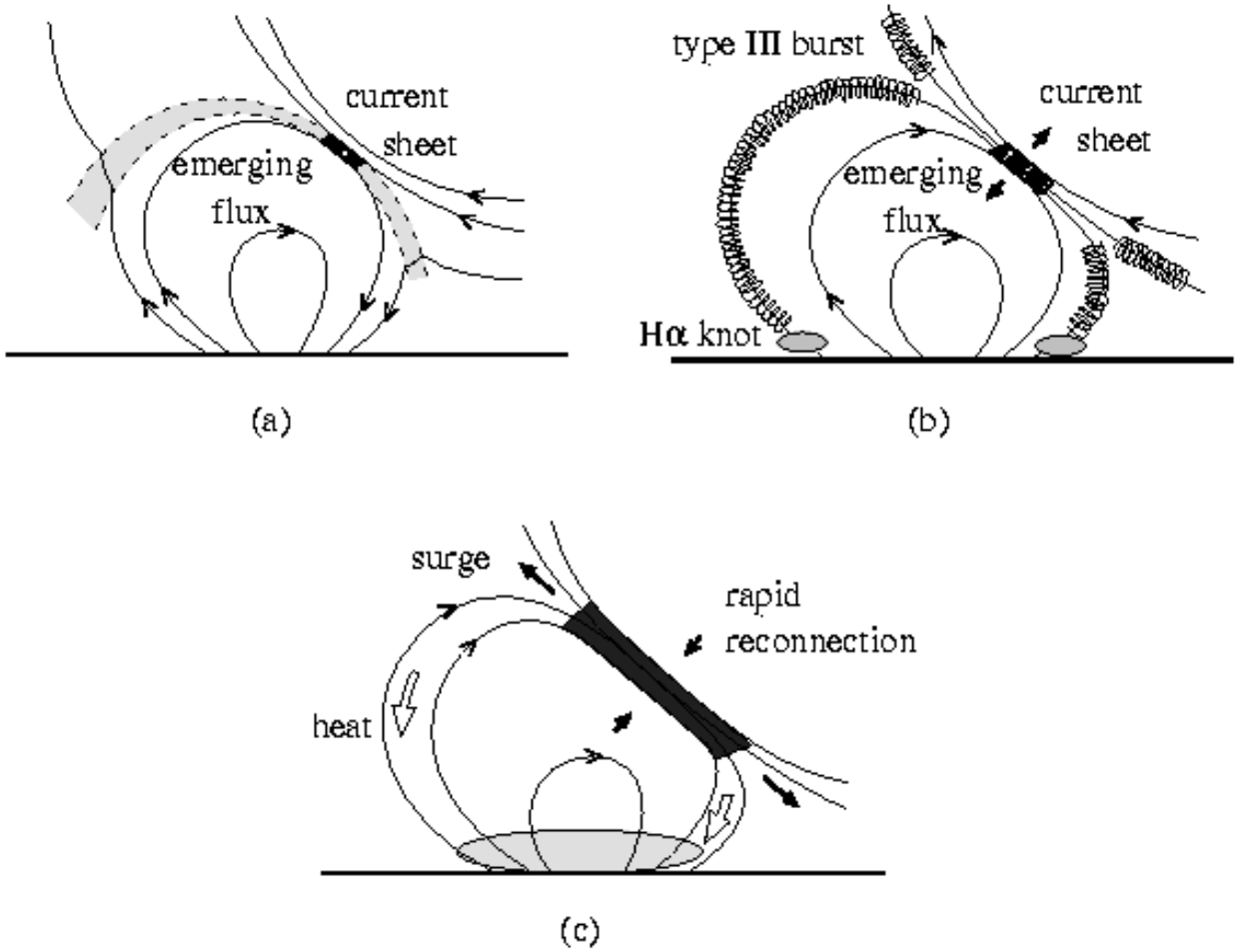

The Emerging Flux Model of Heyvaerts et al. (1977) for a small flare. (a) is the preflare phase when the emerging flux slowly reconnects with the overlying field. Slow-mode shocks (dashed lines) radiate from a small current sheet and heat the plasma that passes through them (striped region). (b) is the impulsive phase caused by the onset of turbulence and anomalous resistivity in the current sheet when it reaches a critical height. The electric field generated by the sudden enhancement in the reconnectionrate accelerates the particles, which produce hard X-rays and type III radio bursts. In the main phase (c) quasi-steady reconnection leads to extensive heating.

Recently there has been considerable interest in three-dimensional reconnection. In this generalization, current sheets are replaced by topologically significant sites in a magnetic field configuration. Attempts to apply 3-D reconnection to flares typically begin with the modelling of the topology of fields in active regions.

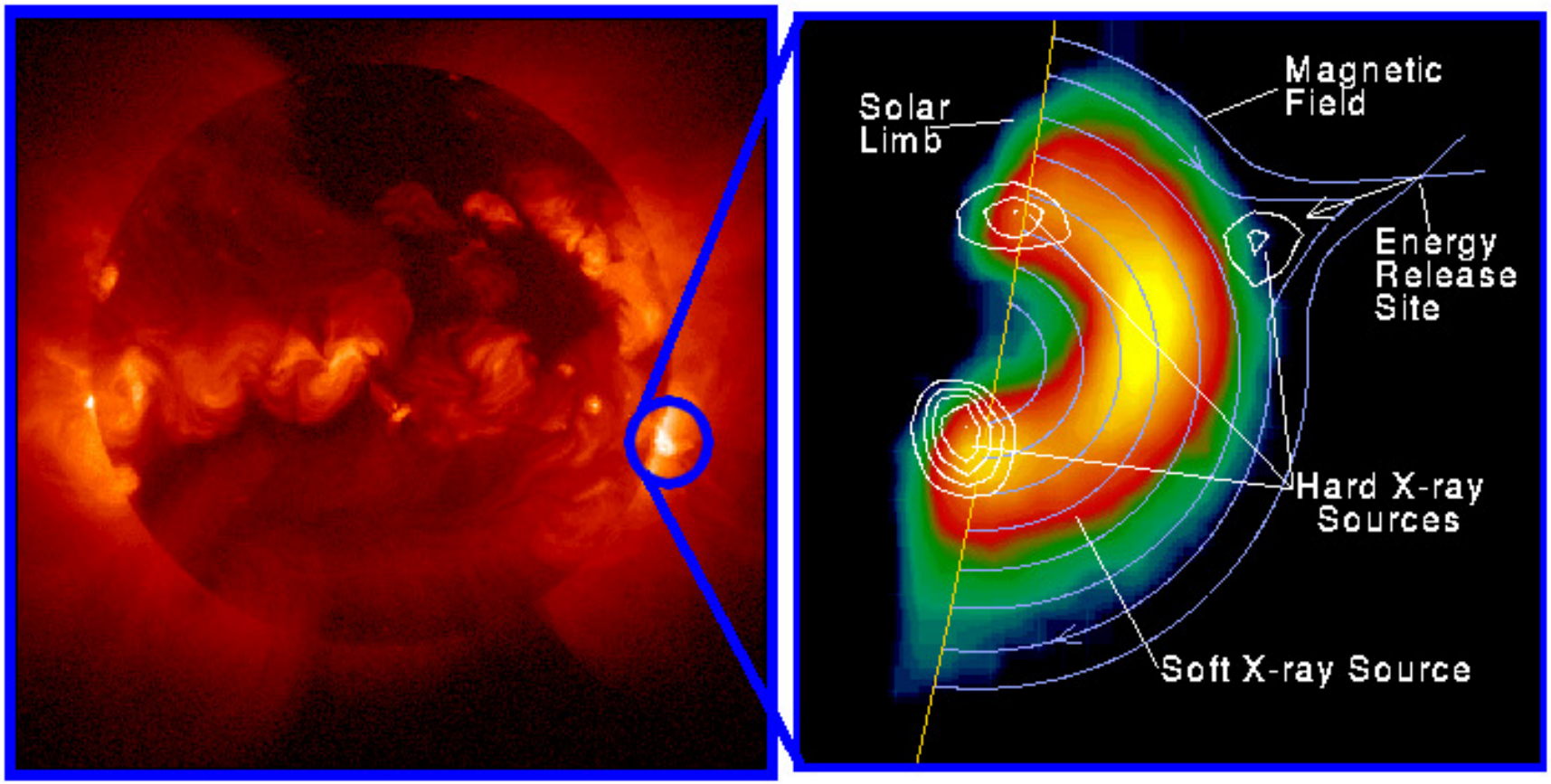

Yohkoh X-ray Image of a Solar Flare, Combined Image in Soft X-rays (left) and Soft X-rays with Hard X-ray Contours (right). Jan 13, 1992.

Reconstruction of a solar flare model from YOHKOH observations of a limb flare.

Recent development – models and observations of "slipping" reconnection: the footpoints of reconnecting magnetic lines "slip" along the flare ribbons of a "J-shape" that is formed by a overlying flux rope (Javier, et al, 2014, ApJ, 788:60, 1)

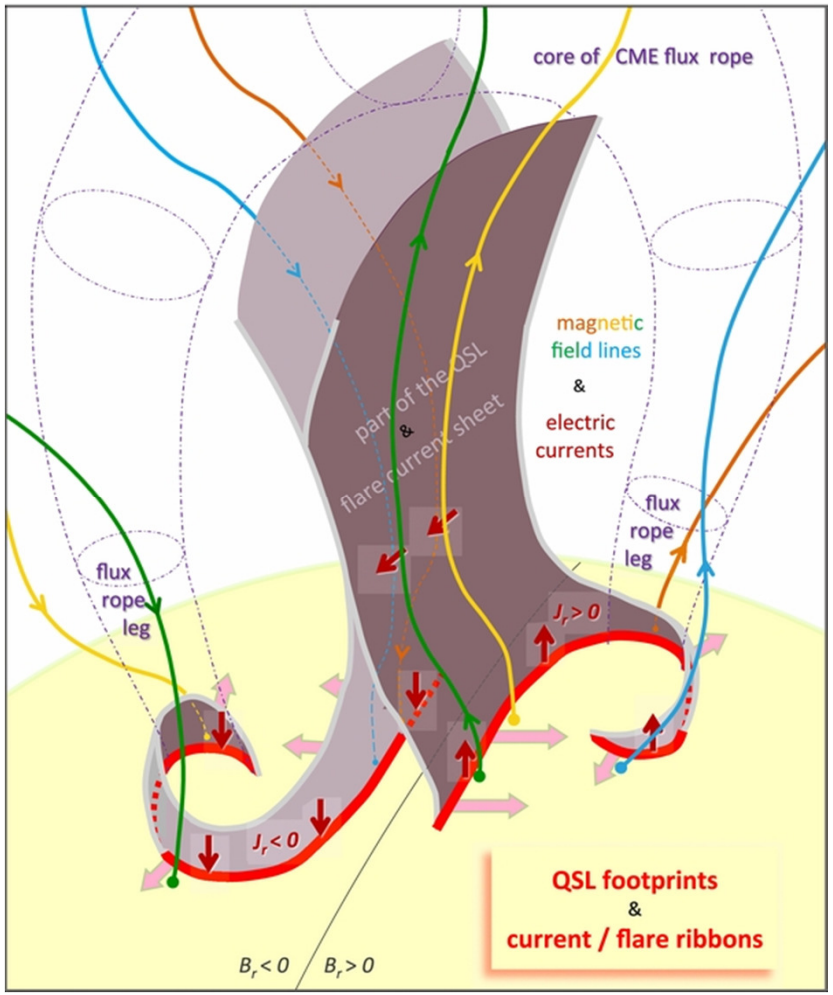

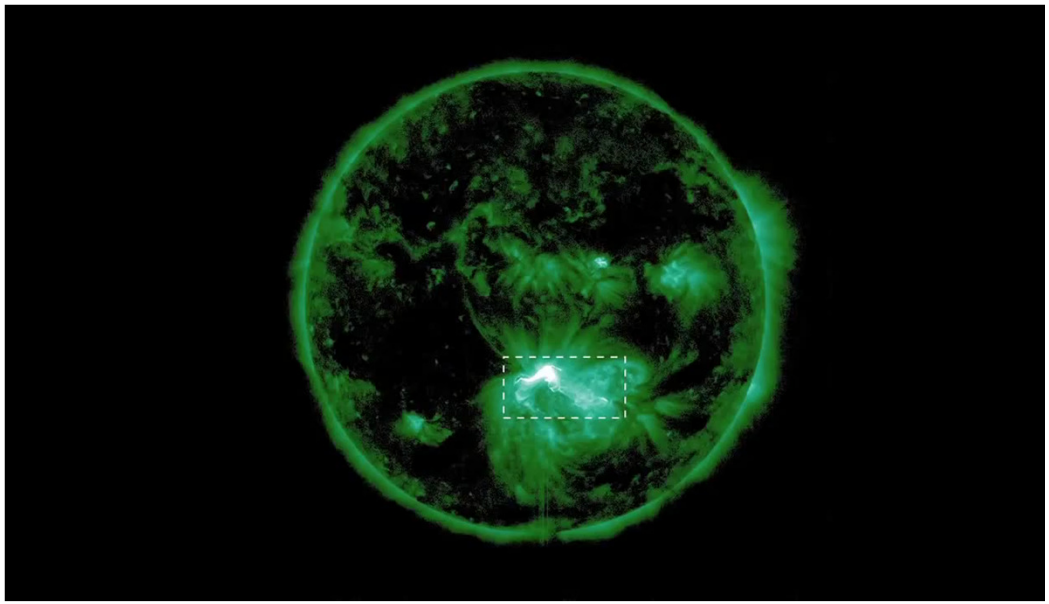

Solar Flares

1. General Observations
2. Theoretical Models Centered on magnetic reconnection
3. **Mechanisms of Particle Acceleration**
4. Flare Observations in Broader Context

Solar flares – outstanding questions

1. How is energy built up and stored?
An X-class flare: 10^{31} - 10^{32} erg, magnetic energy
➔ Magnetic flux emergence, footpoint motion

2. How is energy released explosively?
➔ Magnetic reconnection

3. How are particles accelerated?

The "number problem":
(1) Thick-target flare model:
Requires 10^{37} electrons/s > 20 keV

(2) L = 10 Mm= 10^9 cm, $V = L^3 = 10^{27}$ cm^3, $n = 10^{11}$ cm^{-3}, $N = n\ V$
$=10^{38}$ electrons;
The whole flare region will be depleted in 10 s! – Big puzzle, as flare hard X-ray bursts can last up to ~ 1 hour!

Energization and Particle acceleration mechanisms in solar flares
Magnetic Reconnection is key!

1) Electric Fields // **B**
Hard to maintain large-scale E-field, runaway particles lead to turbulence

2) Shock: 1st order Fermi, as momentum change,

$$\delta p \sim p(u_{\rm sh}/v)$$

the most likely scattering agent is turbulence, so 2nd order energy gain rate:

$$A_{\rm sh} \sim E D_{\rm sc}(u_{\rm sh}/v)^2$$

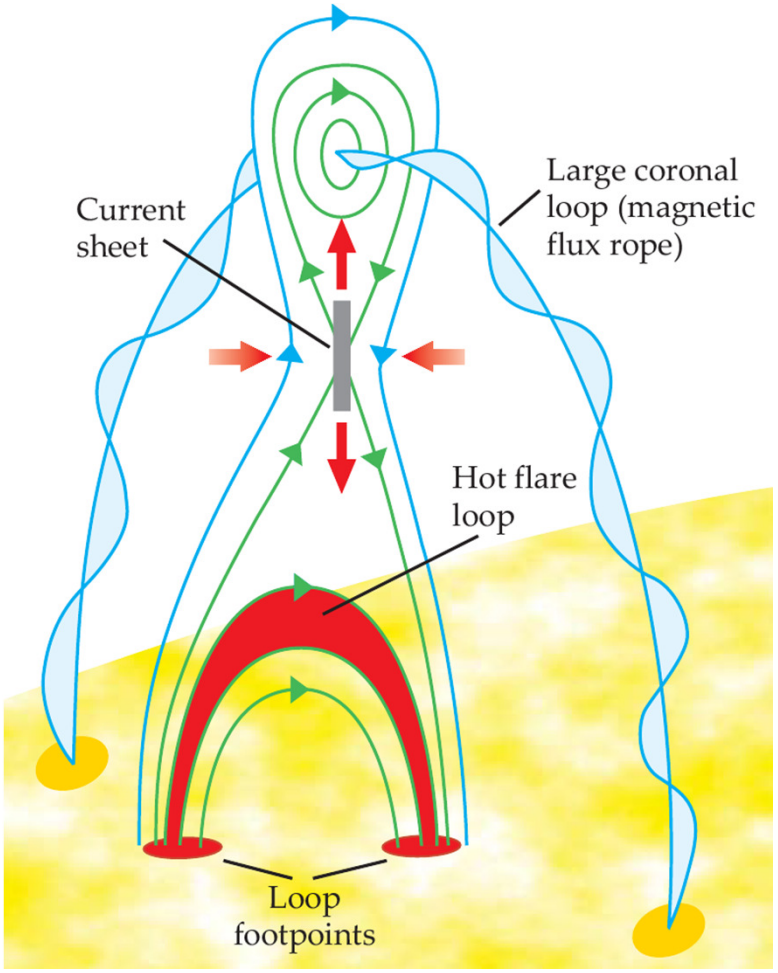

Holman (2012)

3) Stochastic Acceleration (2nd order Fermi) and scattering by turbulence or plasma waves, energy gain rate:

$$A_{\rm SA} \sim E D_{\rm sc}(u_{\rm w}/v)^2$$

Key evidence:
^{3}He enhancement vs. ^{4}He in some solar energetic particles (SEPs; S. Liu+2004,2006)

Mechanisms of Particle Acceleration

There are three main mechanisms of particle acceleration that may work in solar flares:

- direct acceleration by electric field in current sheets
- stochastic acceleration
- acceleration in shock waves
-

Acceleration by electric field – effect of runaway

We consider particle motions in a fully-ionized plasma in an electric field, E:

$$m\frac{d\mathbf{v}}{dt} = -\frac{m\mathbf{v}}{\tau} + e\mathbf{E},$$

where τ is a characteristic time of the loss of momentum due to collisions.

The Coulomb collision time: $$\tau = \frac{1}{nv\Sigma} = \frac{m^2v^3}{nZ^2e^4\Lambda}.$$

$$\frac{dv}{dt} = -\frac{v}{\tau} + \frac{eE}{m} = -\frac{nZ^2e^4\Lambda}{m^2v^2} + \frac{eE}{m}.$$

When $$E > \frac{nZ^2e^3\Lambda}{mv^2} \equiv E_D$$

then there is no stationary mean velocity; the particles continuously accelerates ("run-away electrons"). The critical electric field E_D is called Dreicer field.

The electric field in the reconnection current sheets can exceed E_D.

Stochastic acceleration by plasma turbulence

Consider **stochastic acceleration by fluctuating electric field** (Sturrock, 1966). Considering only one dimension, we may write

$$\frac{dv}{dt} = \frac{d^2x}{dt^2} = \frac{q}{m} E(x,t).$$

We now represent the trajectory of a test particle by

$$x = X(t),$$

so that the equation of motion becomes

$$\frac{d^2X}{dt^2} = \frac{q}{m} E\left(X(t),t\right).$$

We now suppose that the electric field is weak and expand the trajectory in powers of the electric field strength:

$$x = x_0 + v_0 t + X^I(t) + X^{II}(t)...,$$

where x_0 and v_0 are the initial values for x and v.

Substituting the expansion into the equation of motion and separating terms of the equal order we obtain

$$\ddot{X}^I = \frac{q}{m} E(x_0 + v_0 t, t).$$

We assume that the fluctuating electric field is statistically uniform in time and space, so that the correlation (quadratic average)

$$\left\langle E(x,t)E(x+\xi,t+\tau)\right\rangle = \left\langle E^2\right\rangle R(\xi,\tau),$$

where $R(\xi,\tau)$ is the correlation function.

The change in velocity over a time interval t is given, to the first order, by:

$$\Delta\dot{X}^I \equiv \dot{X}^I(t) - \dot{X}^I(0) = \frac{q}{m}\int_0^t dt' E(x_0 + v_0 t', t').$$

Hence,

$$\left\langle (\Delta\dot{X}^I)^2\right\rangle = \frac{q^2}{m^2}\int_0^t dt' \int_0^t dt'' \left\langle E(x_0 + v_0 t', t') E(x_0 + v_0 t'', t'')\right\rangle.$$

Assuming that the time is long compared with the correlation time of the electric field, we obtain

$$\left\langle \frac{(\Delta v)^2}{\Delta t}\right\rangle = \left(\frac{q}{m}\right)^2 \left\langle E^2\right\rangle \int d\tau R(v\tau,\tau).$$

The particle will "diffuse" in velocity space, and can gain high energy.
Stochastic acceleration is a random walk process in the velocity space.

Fermi acceleration

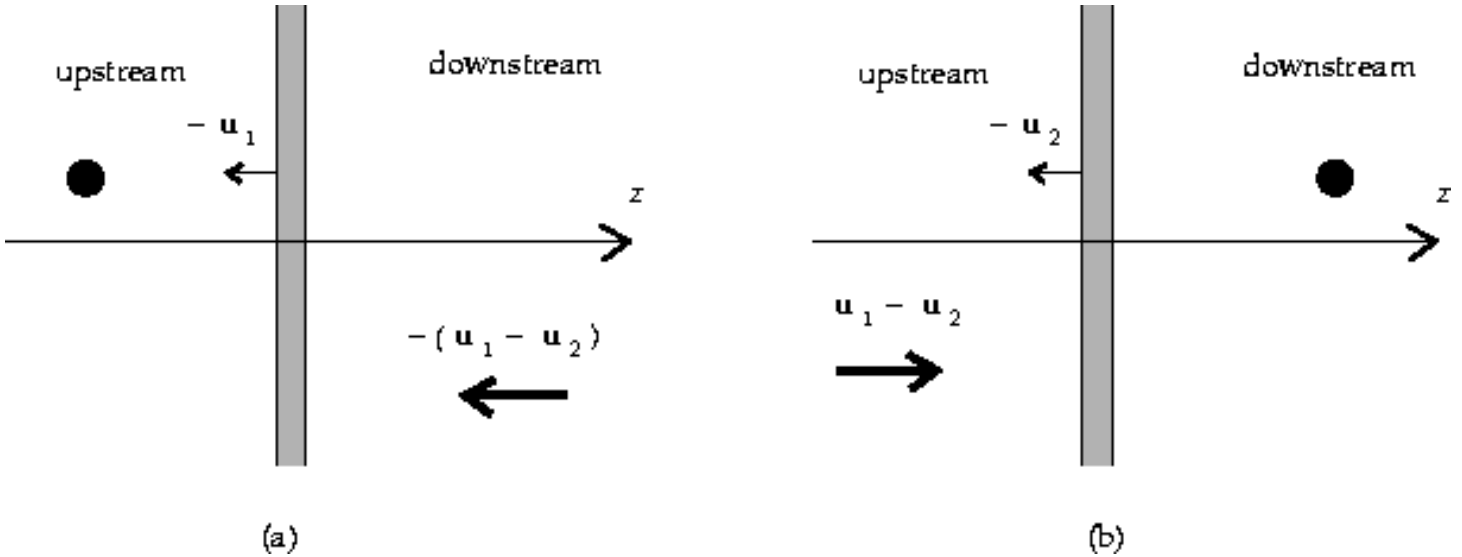

The only important point needed to understand this process is that the fluid velocity changes across the shock. Imagine a fast particle, with speed $v >> u_1$, in the upstream plasma about to cross the shock and enter the downstream plasma. MHD waves can efficiently scatter fast particles, and these waves are convected along with the plasma. MHD waves in the downstream plasma are therefore moving at the fluid speed u_2 , and so our fast particle sees these scattering centers approaching it head on, as shown in figure (a). When the particle enters the downstream plasma and is scattered, its energy is increased because the reflection is head on. In effect the scattering centers act like particles with infinite mass, so that the reflection is analogous to that from a moving wall. Now consider a particle in the downstream plasma about to cross the shock and enter the upstream plasma. As viewed from the downstream plasma, the upstream plasma is flowing toward the particle, as illustrated in figure (b). The scattering centers in the upstream plasma are again approaching the particle. As before, when the particle crosses the shock and is scattered, the scattering is head on and so causes an increase in the particle energy.

粒子加速の標準理論

Fermi Acceleration

(Courtesy of M. Scholer)

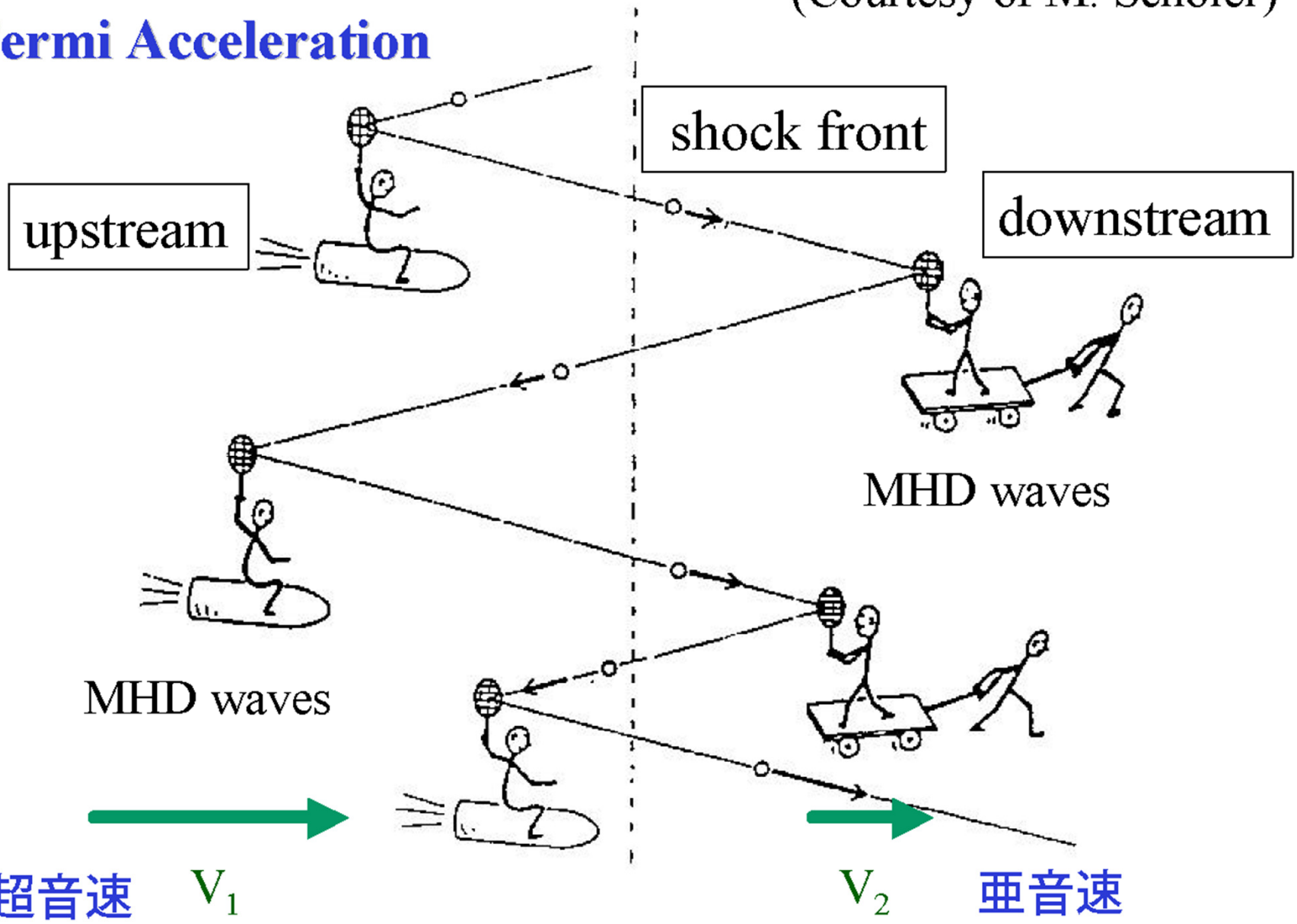

Shock Drift Acceleration

$$\frac{v_\perp^2}{B} = cnst$$

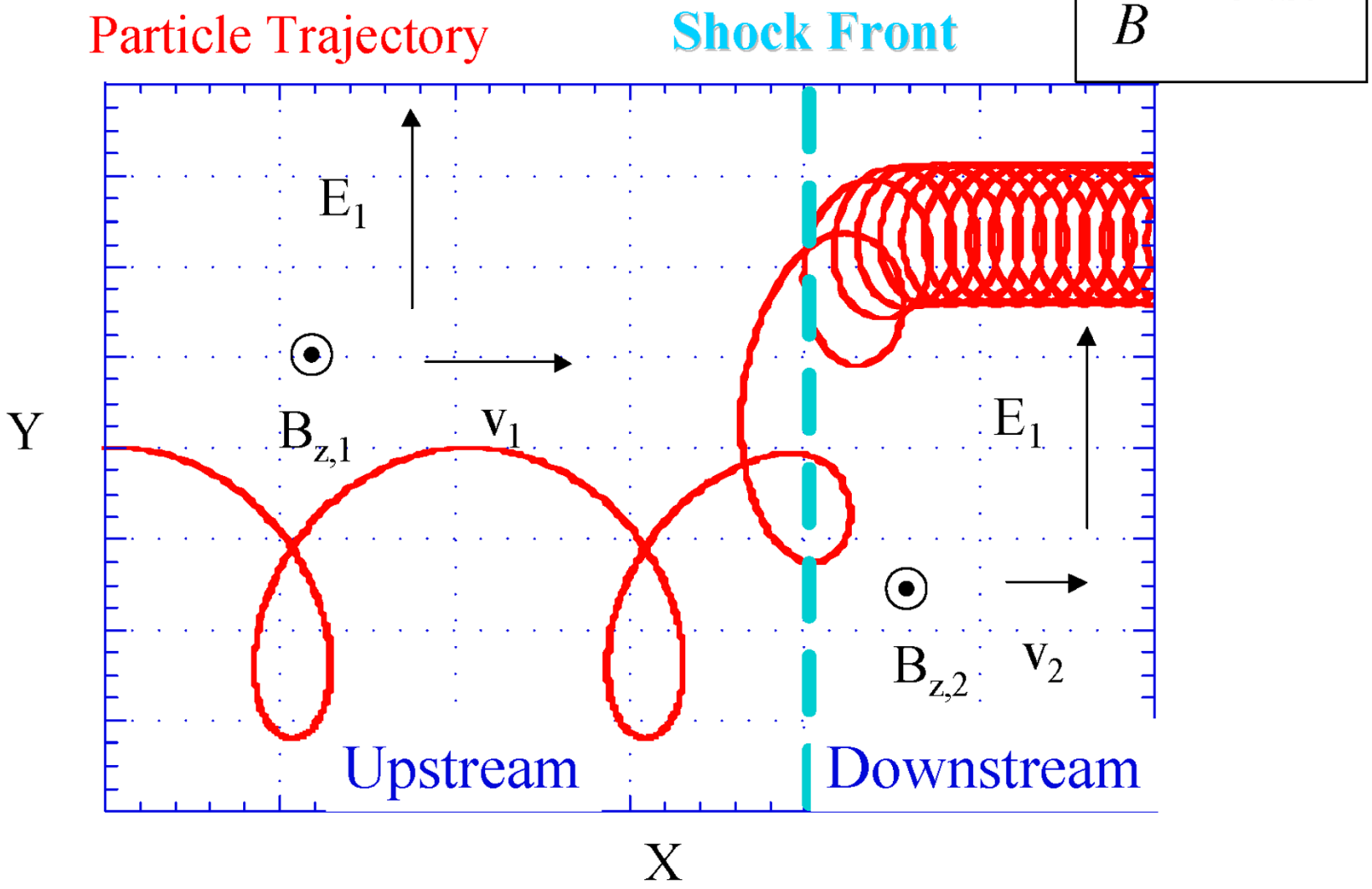

Solar Flares

1. General Observations
2. Theoretical Models Centered on magnetic reconnection
3. Mechanisms of Particle Acceleration
4. **Flare Observations in Broader Context**

Flare radiation and current space missions

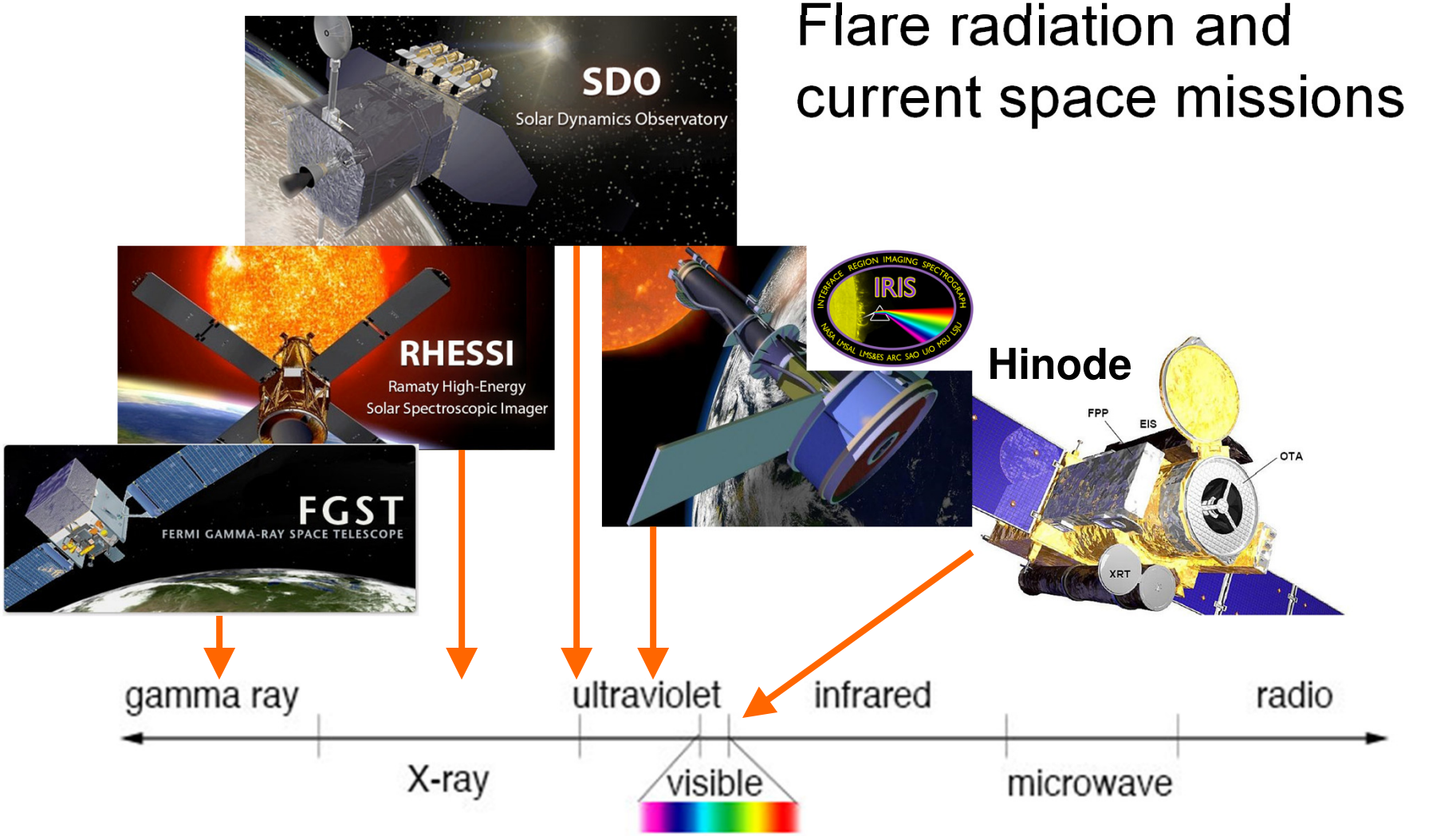

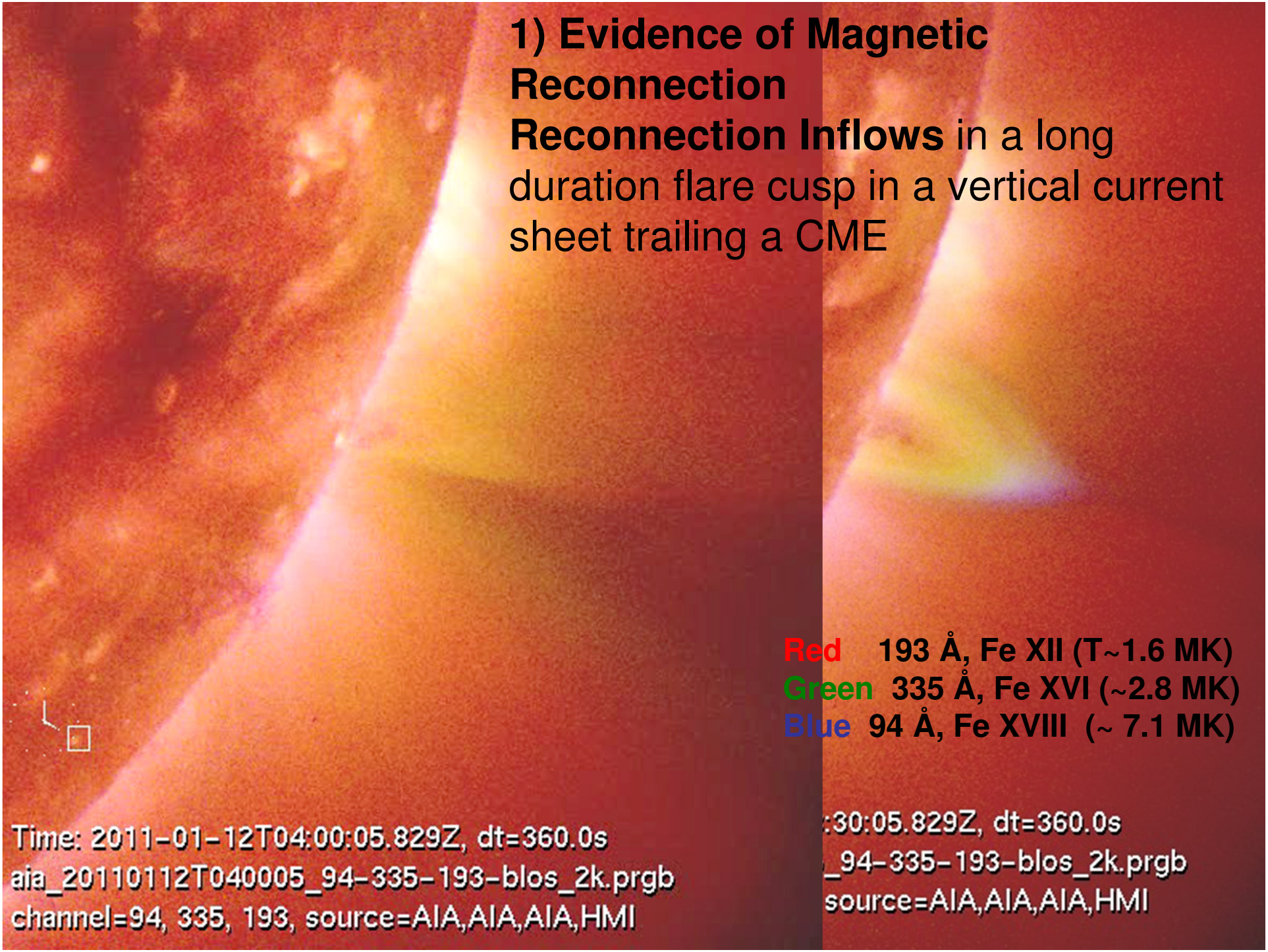
1) Evidence of Magnetic Reconnection
Reconnection Inflows in a long duration flare cusp in a vertical current sheet trailing a CME
Red 193 Å, Fe XII (T~1.6 MK)
Green 335 Å, Fe XVI (~2.8 MK)
Blue 94 Å, Fe XVIII (~ 7.1 MK)
Time: 2011-01-12T04:00:05.829Z, dt=360.0s
aia_20110112T040005_94-335-193-blos_2k.prgb
channel=94, 335, 193, source=AIA,AIA,AIA,HMI
:30:05.829Z, dt=360.0s
_94-335-193-blos_2k.prgb
source=AIA,AIA,AIA,HMI

Reconnection inflows in space-time, v_{in}=4 km/s, v_A~1000 km/s,
Reconnection rate:
v_{in}/v_A=0.004

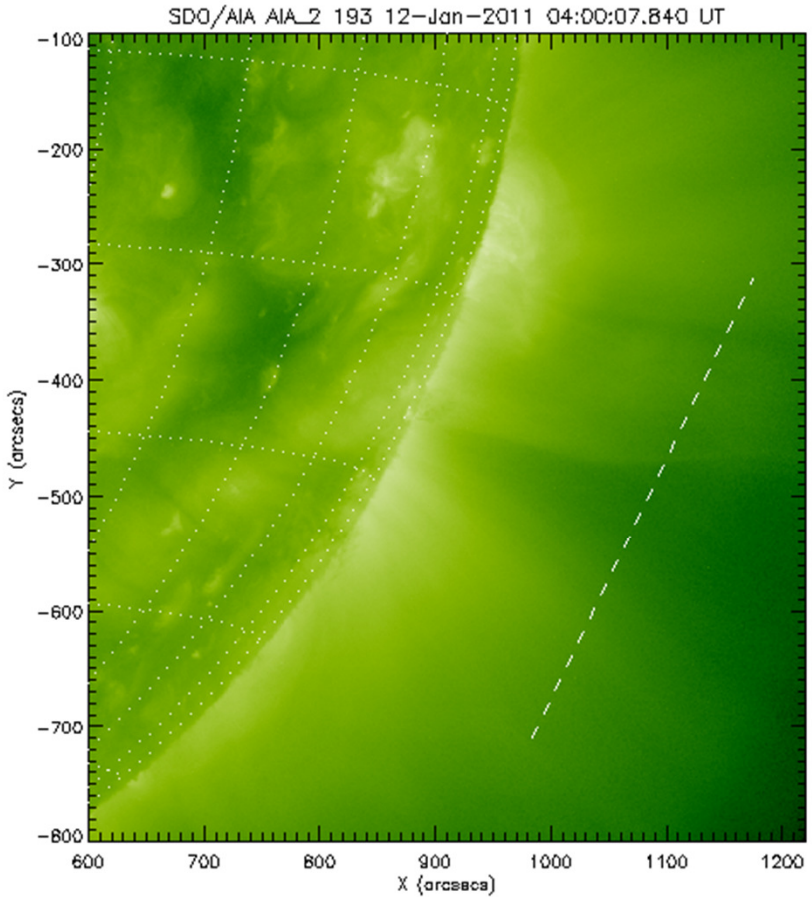

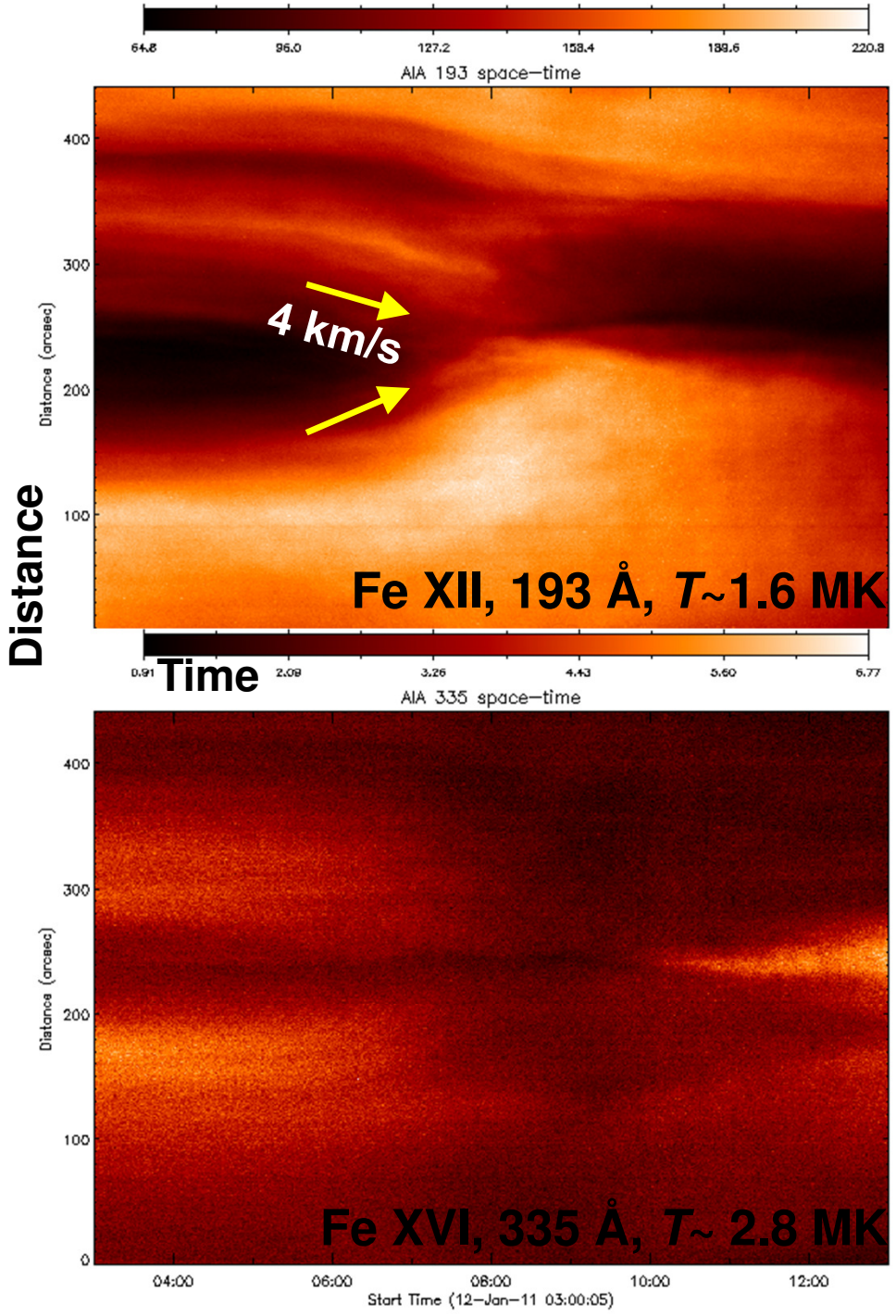

Bi-directional reconnection outflows: plasmoid ejections, contracting loops (Liu et al. 2013)

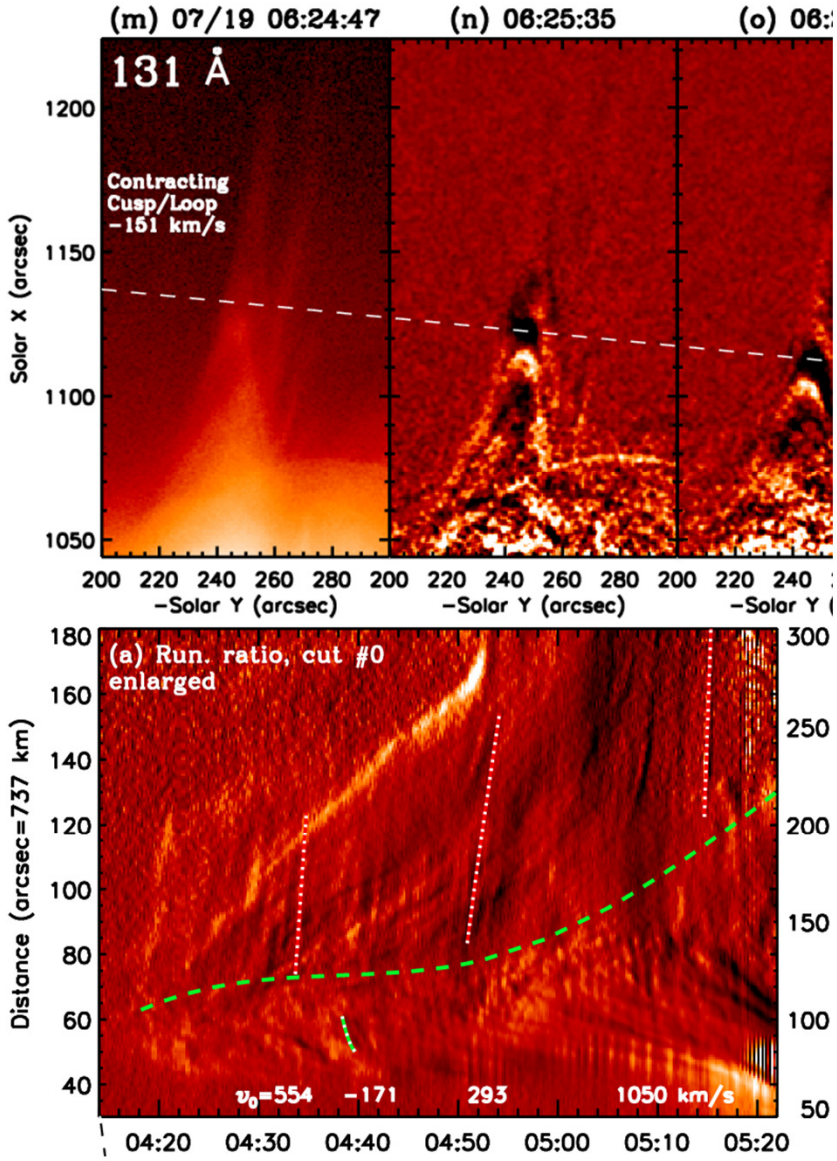

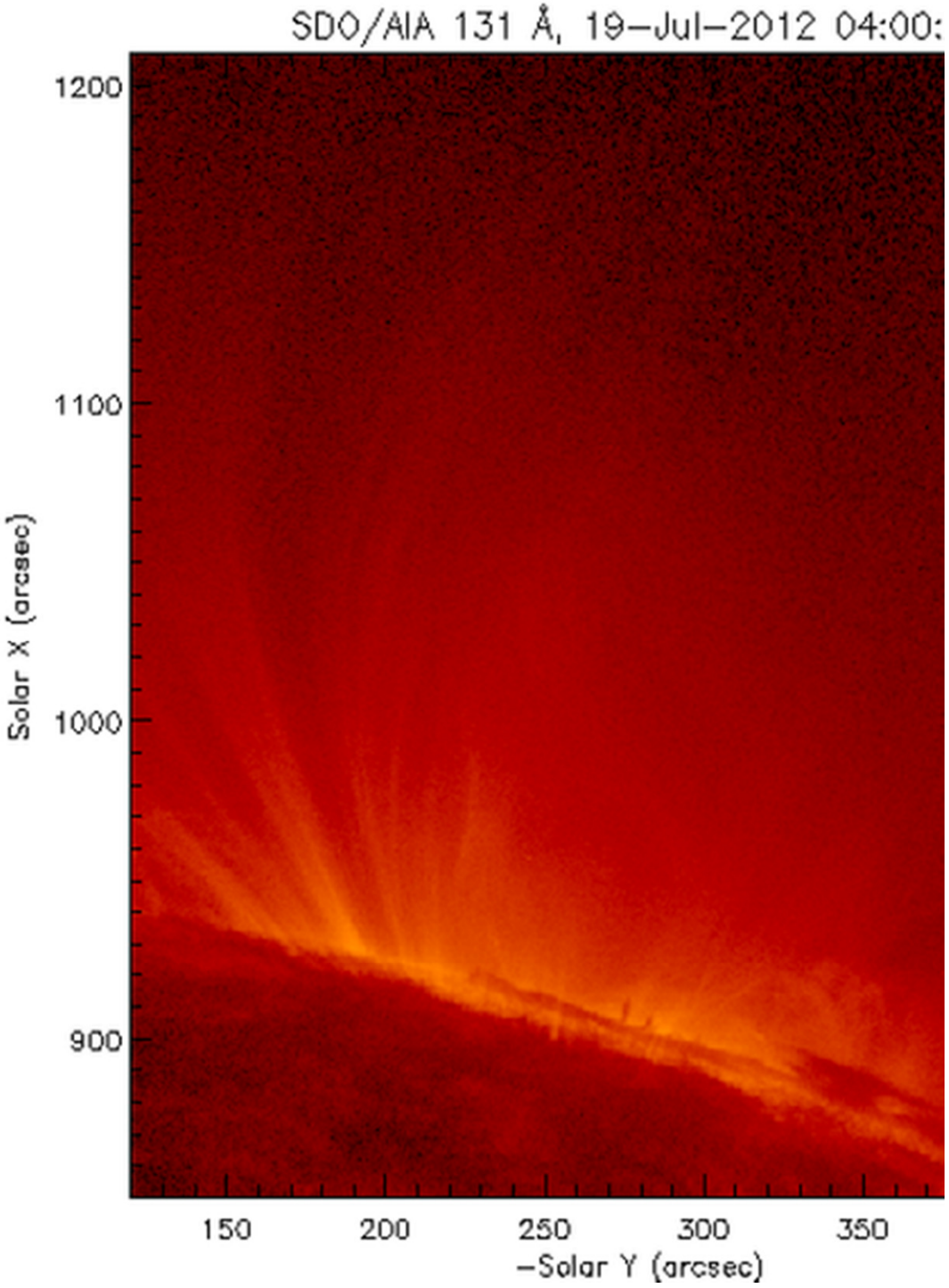

“Turbulent” reconnection outflows – flares tadpoles: supra-arcade downflows (SADs; e.g., McKenzie+2013; Liu+2013; ApJ)

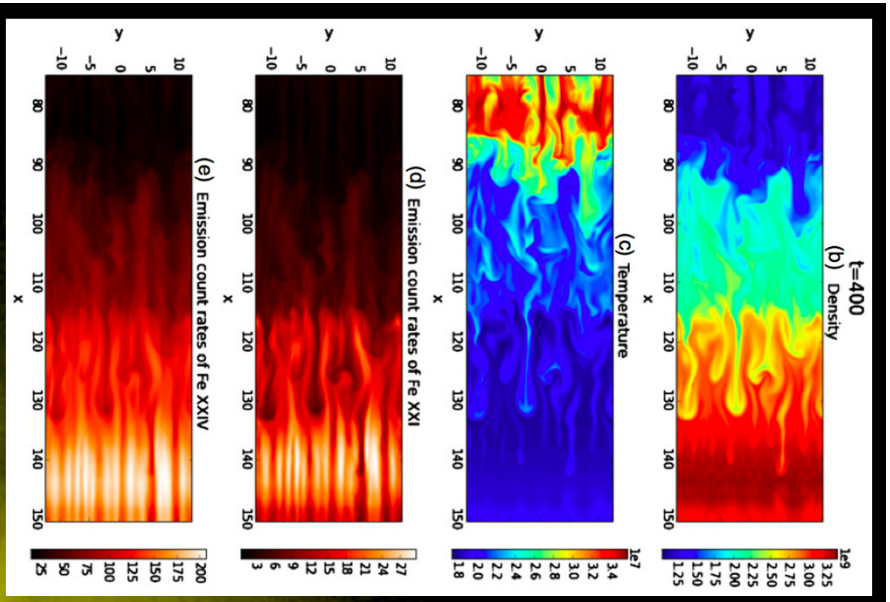

, dt=24.0s

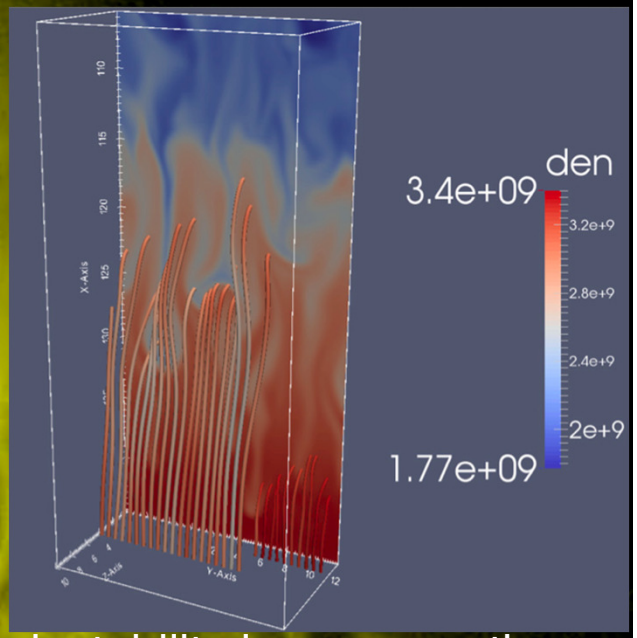

Rayleigh-Taylor instability in reconnection exhausts (Guo, Huang et al. 2014 ApJ; cf. Cassak et al. 2013 ApJ)

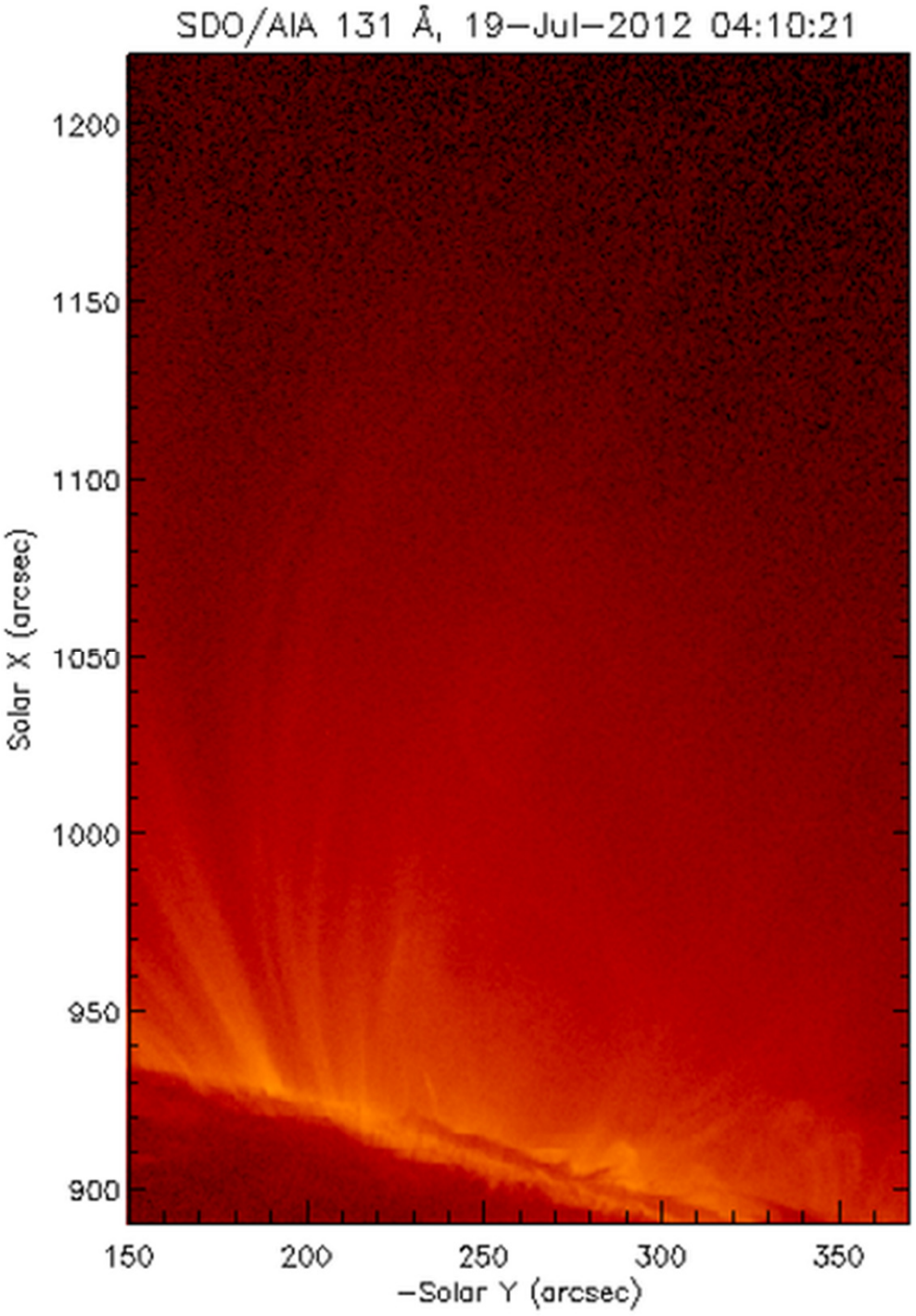

RHESSI contours on AIA 131 Å

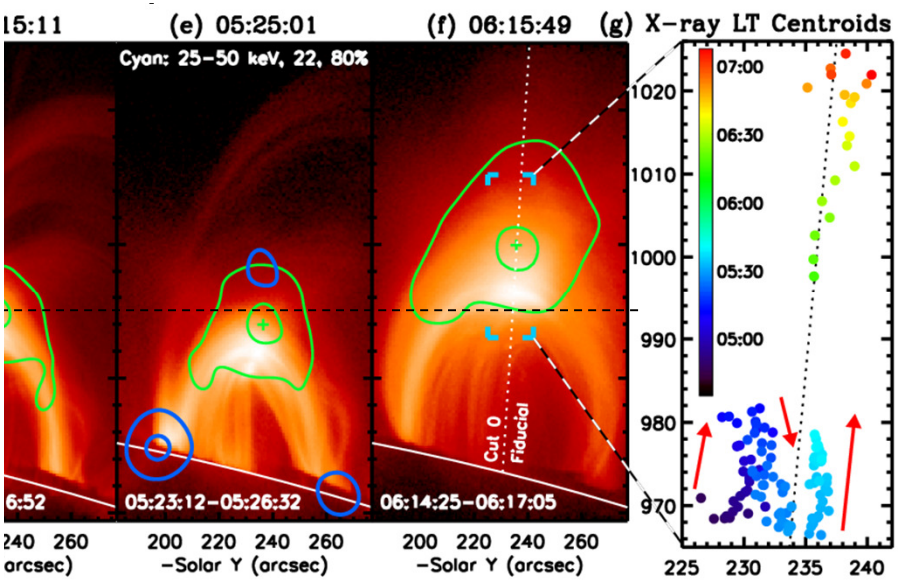

Above-the-loop-top source (e.g., Masuda 1994): Evidence of stochastic acceleration, turbulence can trap and accelerate particles

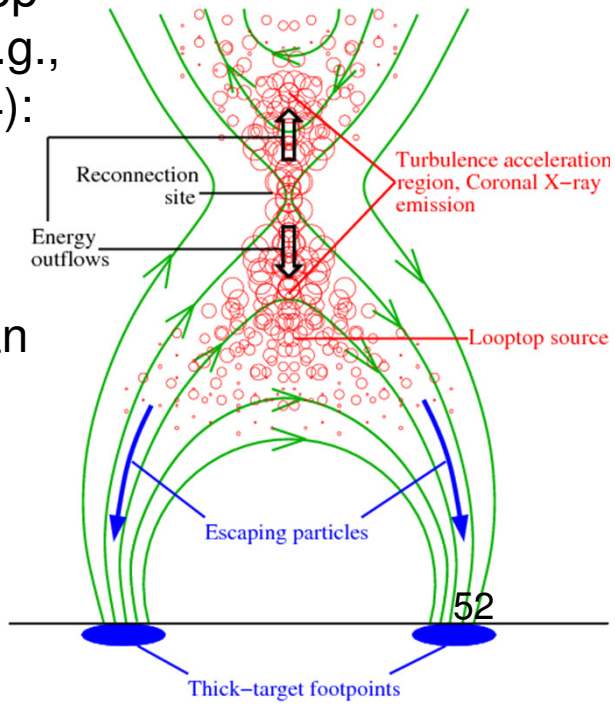

Heating + acceleration in reconnection outflow regions

Temperature map

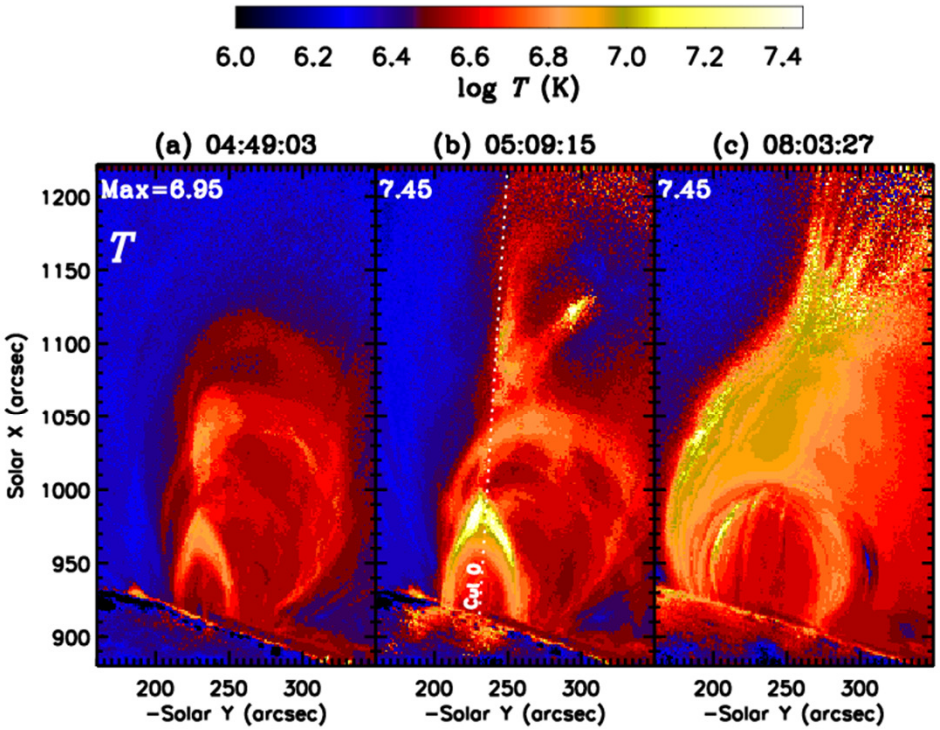

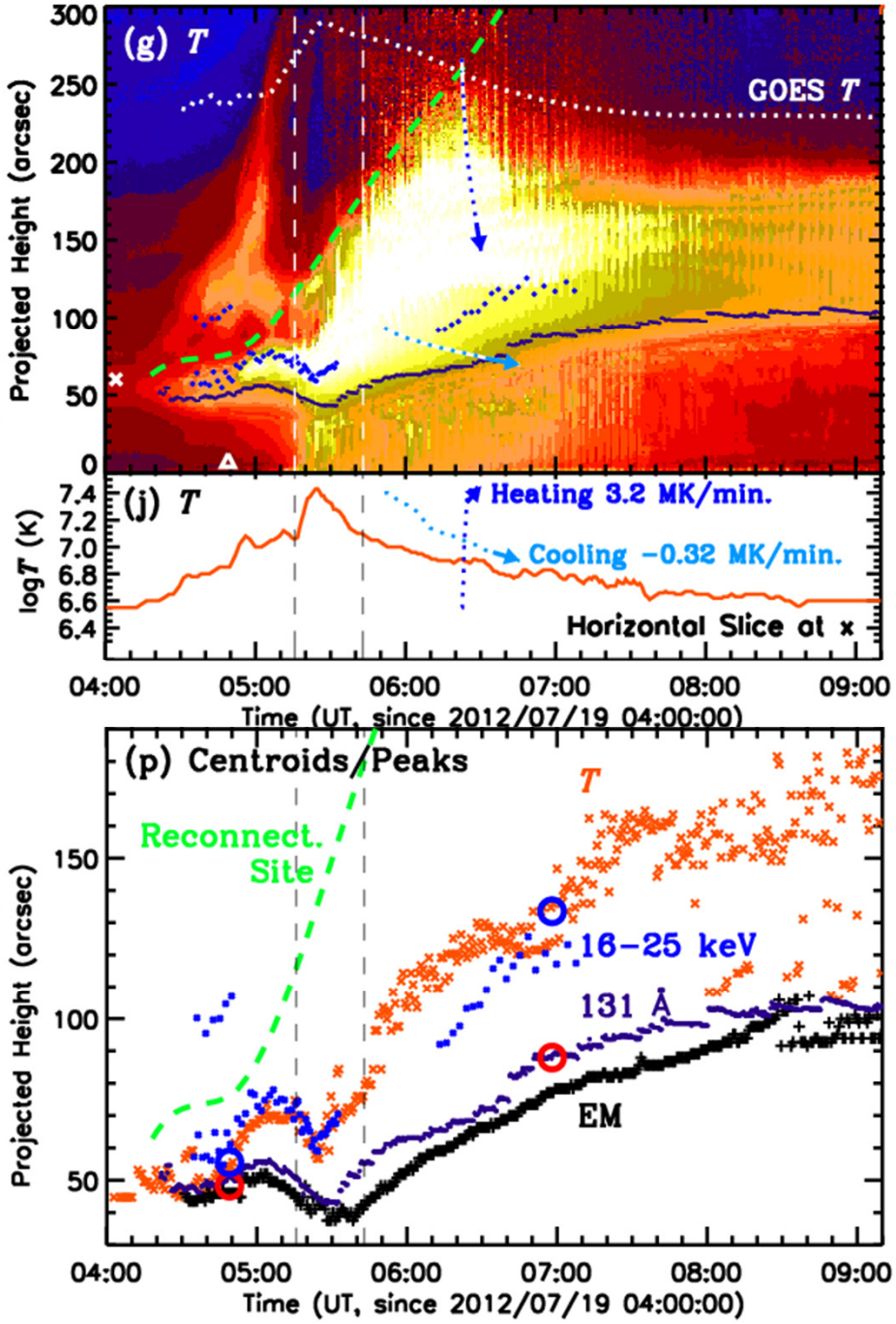

- HXR Centroid near EM peak, below highest-T region that is again below the reconnection site

2) Chromospheric Evaporation

Leg emission and its upward motion along loop – imaging chromospheric evaporation

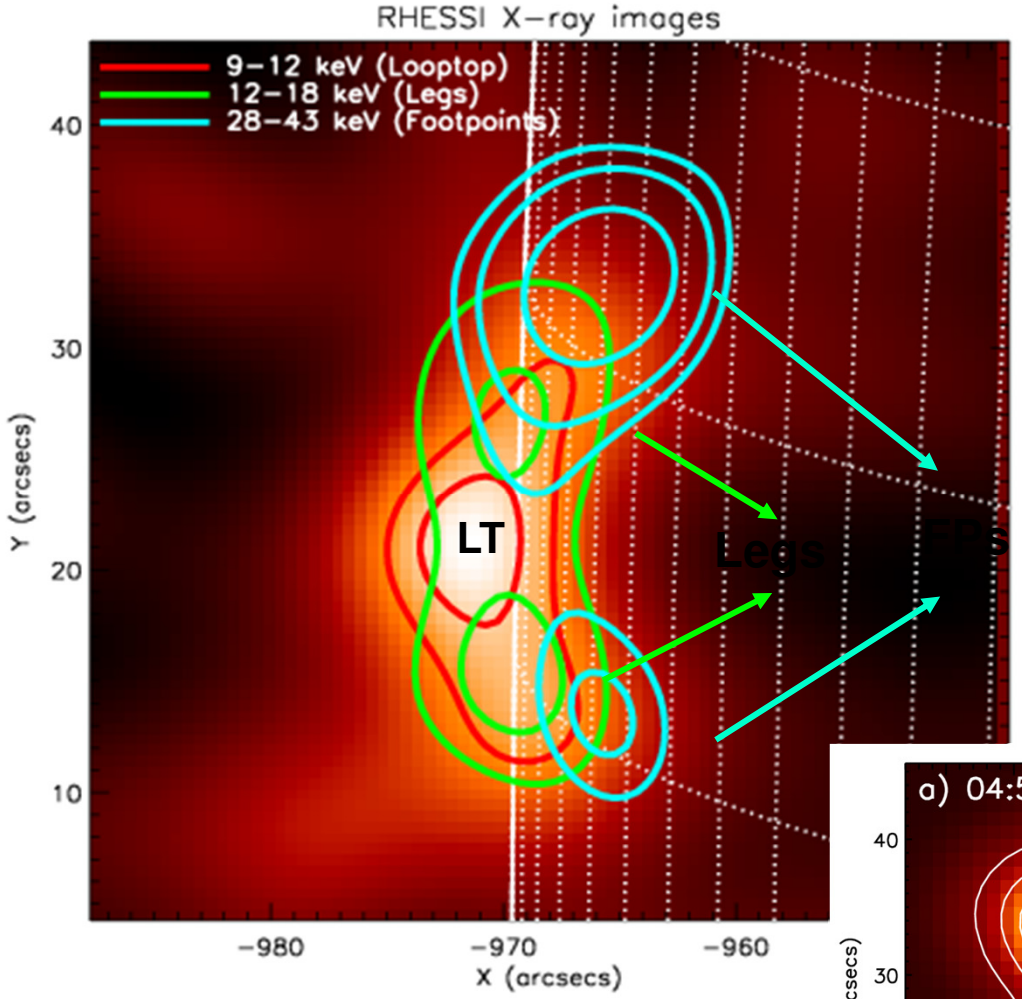

(Liu et al. 2006, ApJ)

high-density loop resulting from chromospheric evaporation

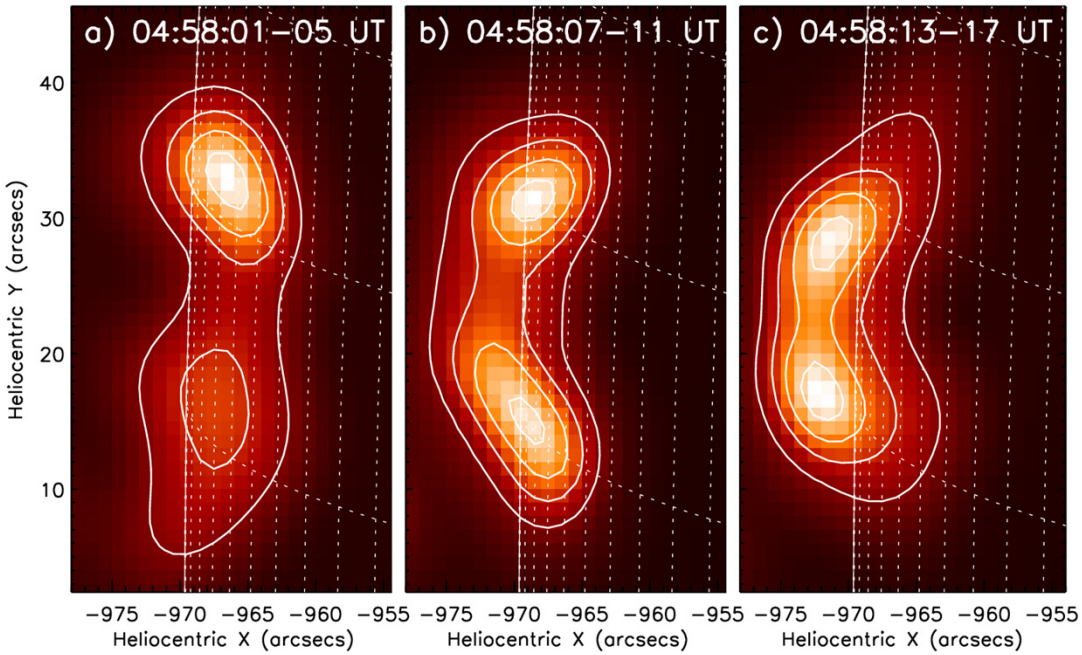

Coupling Result: Hydrodynamics

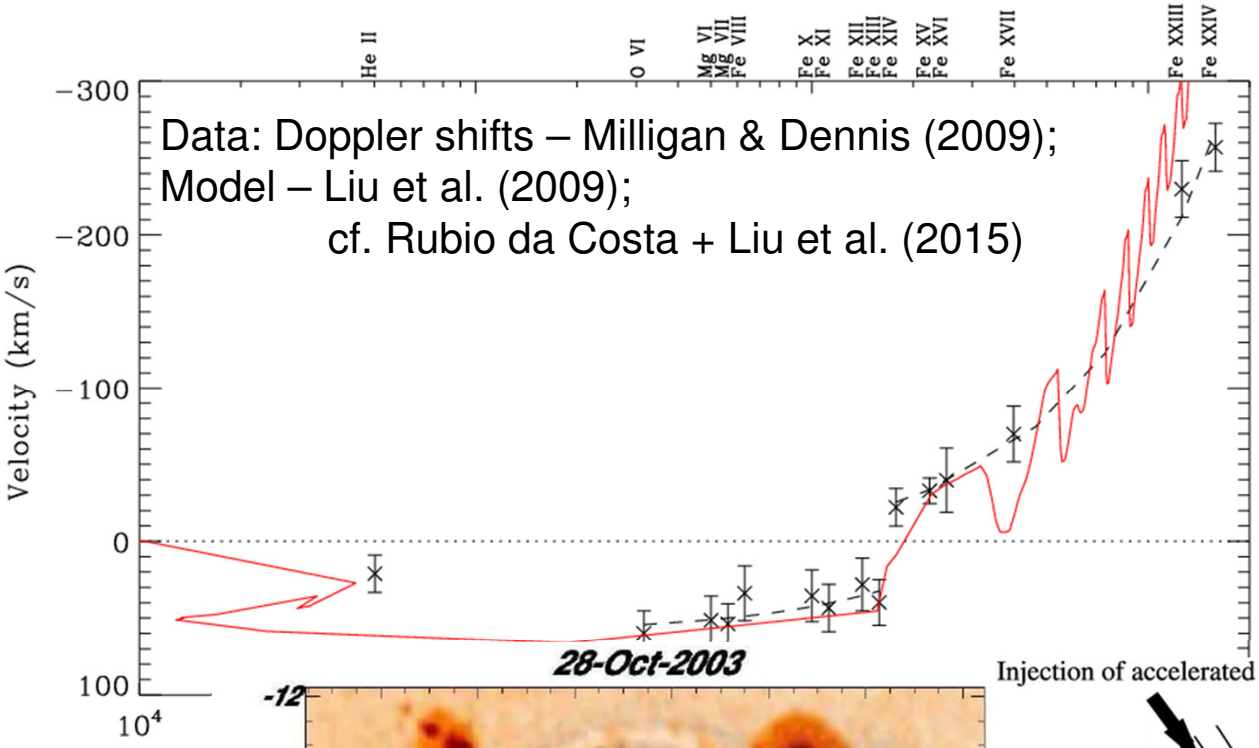

Simulations fit observed temperature distribution of up- and downflow velocities

Downward pressure pulse – flare triggered sunquakes

(Kosovichev 2006)

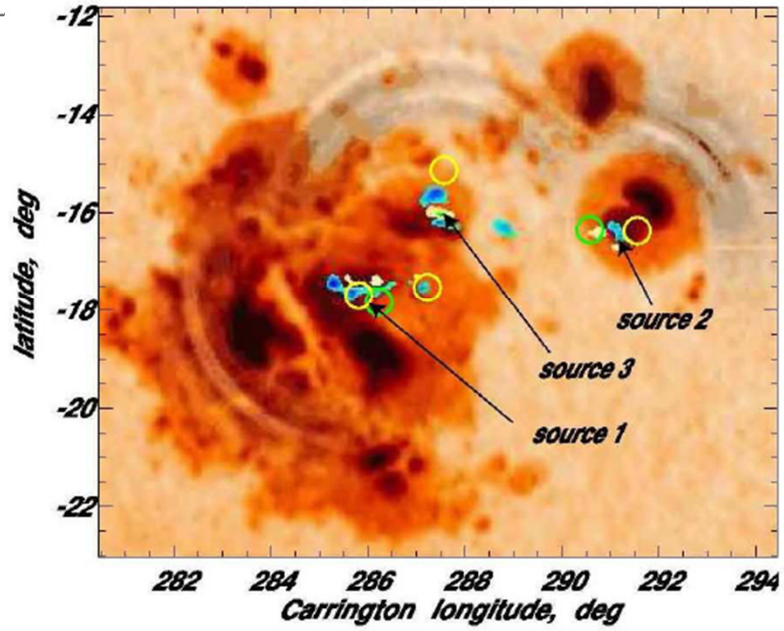

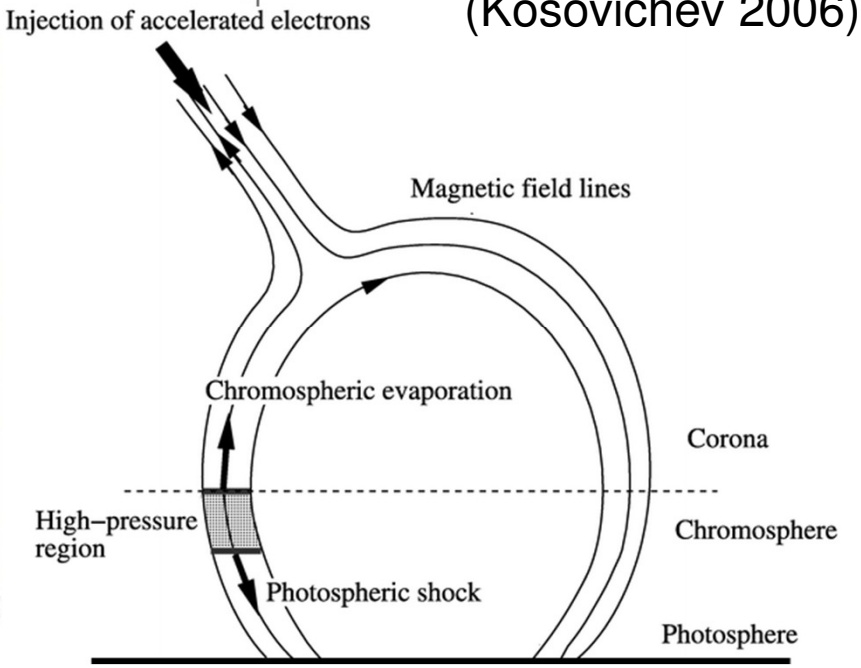

IRIS (Interface Region Imaging Spectrograph, June 2013)

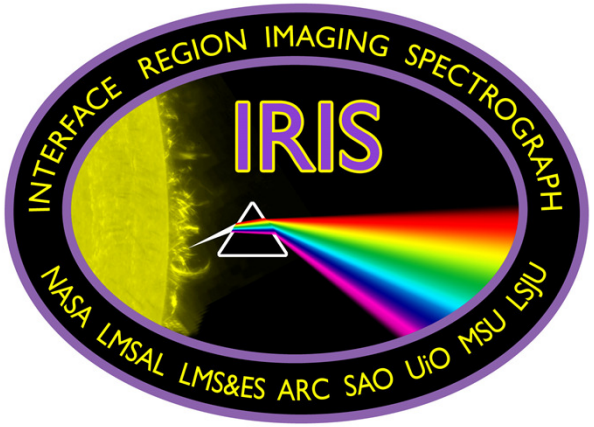

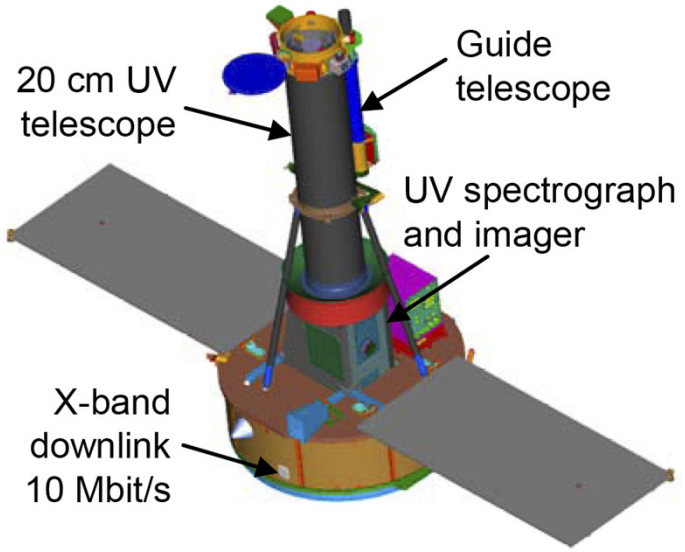

IRIS Observations of an X-class flare (H. Tian+ 2015, ApJ

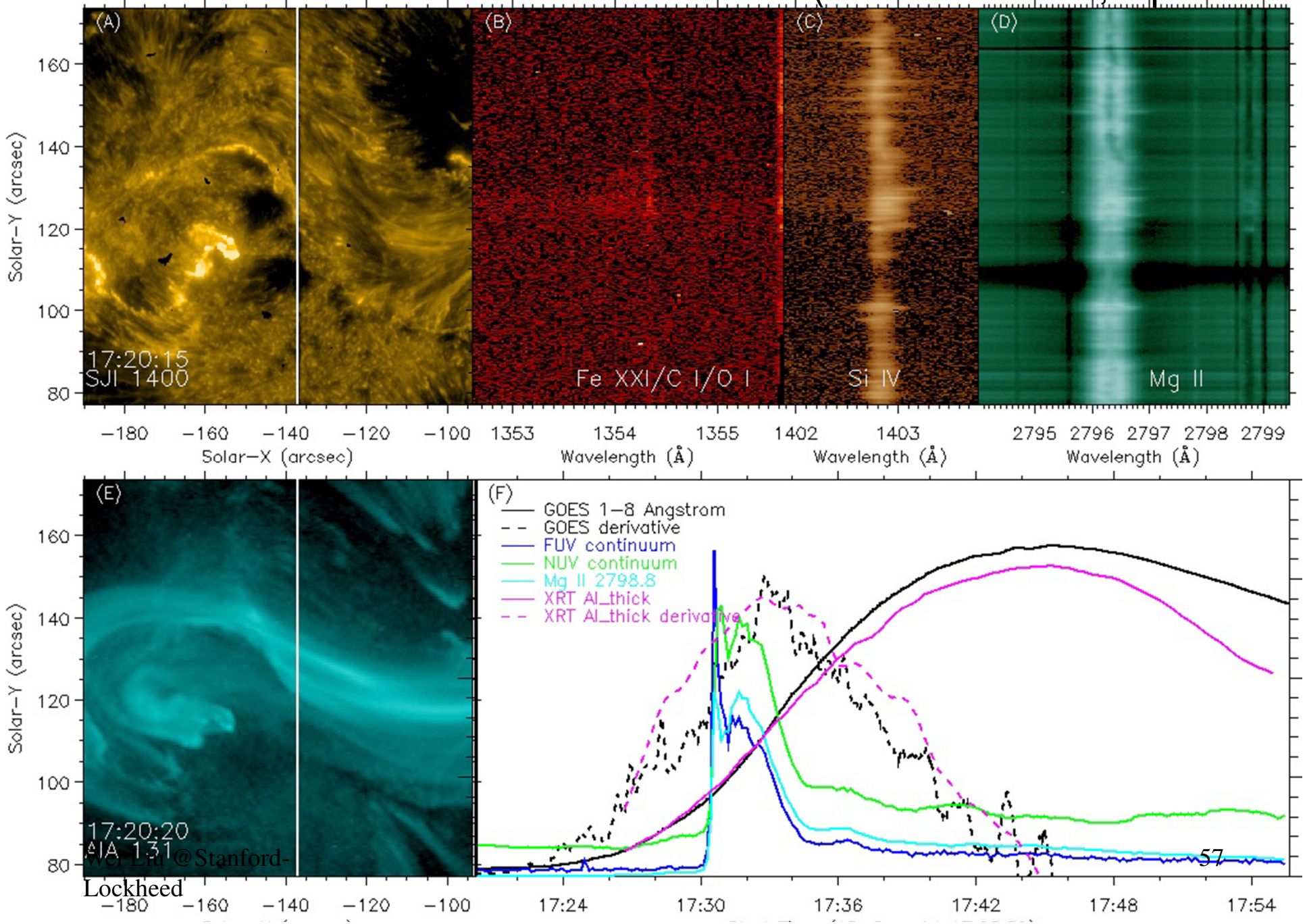

Solar flares and other high-energy processes in the universe